

STUDY OF MEGAKARYOCYTES AND PLATELETS IN BERNARD SOULIER SYNDROME  
USING PATIENT INDUCED PLURIPOTENT STEM CELLS



A Dissertation Submitted in Partial Fulfillment of the Requirements  
for the Degree of Doctor of Philosophy in Biomedical Sciences  
Inter-Department of Biomedical Sciences  
Graduate School  
Chulalongkorn University  
Academic Year 2018  
Copyright of Chulalongkorn University

การศึกษาเซลล์ต้นกำเนิดเกล็ดเลือดและเกล็ดเลือดในผู้ป่วยกลุ่มอาการเบอร์นาร์ตซูเลียร์โดยอินดิวิช  
พลุรีโพเทนท์สเต็มเซลล์ของผู้ป่วย



วิทยานิพนธ์นี้เป็นส่วนหนึ่งของการศึกษาตามหลักสูตรปริญญาวิทยาศาสตรดุษฎีบัณฑิต  
สาขาวิชาชีวเวชศาสตร์ สหสาขาวิชาชีวเวชศาสตร์  
บัณฑิตวิทยาลัย จุฬาลงกรณ์มหาวิทยาลัย  
ปีการศึกษา 2561  
ลิขสิทธิ์ของจุฬาลงกรณ์มหาวิทยาลัย



พรทิพย์ เมฆฉาย : การศึกษาเซลล์ต้นกำเนิดเกล็ดเลือดและเกล็ดเลือดในผู้ป่วยกลุ่มอาการเบอร์นาร์ตซูลิเยร์ โดยอินดิฟิวชันพลาซมาเซลล์ของผู้ป่วย. ( STUDY OF MEGAKARYOCYTES AND PLATELETS IN BERNARD SOULIER SYNDROME USING PATIENT INDUCED PLURIPOTENT STEM CELLS) อ.ที่ปรึกษาหลัก : ศ. ดร. นพ.พลภัทร โรจนนครินทร์

กลุ่มอาการเบอร์นาร์ตซูลิเยร์เป็นความผิดปกติที่ถ่ายทอดทางพันธุกรรม มีความผิดปกติในการสร้างเกล็ดเลือดได้จำนวนน้อยและมีเกล็ดเลือดขนาดใหญ่ สาเหตุเกิดจากความผิดปกติของ GPIb-IX-V complex ซึ่งกลไกในการสร้างเกล็ดเลือดขนาดใหญ่นั้นยังไม่ชัดเจน ปัจจุบันเซลล์ megakaryocytes (MKs) สามารถสร้างได้จากอินดิฟิวชันพลาซมาเซลล์เพื่อนำมาศึกษากระบวนการสร้างเกล็ดเลือดโดยใส่ยา สารเคมี หรือ เปลี่ยนแปลงทางพันธุกรรม ในการศึกษาวิจัยได้สร้างอินดิฟิวชันพลาซมาเซลล์จากผู้ป่วยสองรายที่มีการกลายพันธุ์ในยีนที่ต่างกัน (แทนผู้ป่วยที่มีการกลายพันธุ์ในยีน *GP1BA* และ *GP1BB* ด้วย BSS-A และ BSS-B ตามลำดับ) จากนั้นทำการเปลี่ยนแปลงให้เป็นเซลล์ MKs และเกล็ดเลือดในหลอดทดลอง เกล็ดเลือดที่ได้จะถูกนำมาแยกและวัดขนาดเส้นผ่านศูนย์กลางวงแหวน tubulin พบว่าเกล็ดเลือดของผู้ป่วยมีการสร้าง proplatelet ที่ผิดปกติในส่วนปลายและก้านที่หนา รวมถึงเกล็ดเลือดมีขนาดใหญ่ขึ้นอย่างมีนัยสำคัญทางสถิติ การเพิ่มการแสดงออกของไกลโคโปรตีน Ib โดยการใส่ lentivirus ที่มียีน *GP1BA* เข้าไปในอินดิฟิวชันพลาซมาเซลล์ของผู้ป่วย พบว่าสามารถเปลี่ยนแปลงโครงสร้างของ proplatelet ให้เป็นปกติ รวมถึงมีขนาดเกล็ดเลือดลดลง แต่ไม่มีการแสดงออกของยีนในผู้ป่วย BSS-B นอกจากนี้ยังได้ทำการศึกษากลไกการเกิดเกล็ดเลือดขนาดใหญ่โดยใช้ไซโตไคน์  $IL-1\alpha$  และยา blebbistatin พบว่า  $IL-1\alpha$  สามารถเหนี่ยวนำให้เกิดเกล็ดเลือดขนาดใหญ่ในกลุ่มปกติแต่ไม่ส่งผลต่อเกล็ดเลือดของผู้ป่วยให้ใหญ่ขึ้น และเมื่อศึกษา blebbistatin ที่ออกฤทธิ์ยับยั้งการทำงานของโปรตีน myosin II พบว่าสามารถลดขนาดของเกล็ดเลือดของผู้ป่วยได้อย่างมีนัยสำคัญทางสถิติ การใส่ยา blebbistatin และ  $IL-1\alpha$  ร่วมกันส่งผลให้ค่าเฉลี่ยของขนาดเกล็ดเลือดผู้ป่วยลดลงอย่างมีนัยสำคัญทางสถิติ ในงานวิจัยนี้ผู้ทดลองยังได้ทำการสร้างอินดิฟิวชันพลาซมาเซลล์ที่มีโปรตีน tubulin เชื่อมต่อกับโปรตีนเรืองแสงสีเขียว ซึ่งสามารถนำมาใช้เป็นเครื่องมือศึกษาในแบบจำลองการเกิดโรคเกล็ดเลือดได้ในอนาคต โดยสรุป อินดิฟิวชันพลาซมาเซลล์ของผู้ป่วยกลุ่มอาการเบอร์นาร์ตซูลิเยร์เป็นแบบจำลองที่ดีสำหรับโรคเกล็ดเลือดขนาดใหญ่ โดยผลที่ได้จากการศึกษาแสดงให้เห็นว่า GPIb-IX-V ไม่จำเป็นสำหรับการเหนี่ยวนำการสร้างเกล็ดเลือดโดย  $IL-1\alpha$  แต่ทำให้เกิด การสร้าง proplatelet ที่ผิดปกติโดยเกี่ยวข้องกับการทำงานของ myosin

สาขาวิชา ชีวเวชศาสตร์

ลายมือชื่อนิสิต .....

ปีการศึกษา 2561

ลายมือชื่อ อ.ที่ปรึกษาหลัก .....

# # 5587841720 : MAJOR BIOMEDICAL SCIENCES

KEYWORD: Induced pluripotent stem cells Bernard Soulier syndrome Megakaryocytes Platelets  
Macrothrombocytopenia

Ponthip Mekchay : STUDY OF MEGAKARYOCYTES AND PLATELETS IN BERNARD SOULIER SYNDROME USING PATIENT INDUCED PLURIPOTENT STEM CELLS. Advisor: Prof. Pontapat Rojnuckarin, M.D. Ph.D.

Bernard-Soulier syndrome (BSS) is a hereditary macrothrombocytopenia caused by defects in GPIb-IX-V complex. The mechanism of large platelet formation remains unclear. Currently, megakaryocytes (MKs) can be generated from induced pluripotent stem cells (iPSCs) to study platelet production under pharmacologic or genetic manipulations. In this study, we generated iPSC lines from 2 patients with mutations in different genes (*GP1BA* and *GP1BB*: termed BSS-A and BSS-B, respectively), iPSCs were then differentiated into MKs and platelets. *In vitro* iPSCs-derived platelets were stained for circumferential tubulin and measured the diameters (N = 500 per condition). BSS-iPSCs produced abnormal proplatelets with thick shafts and tips, as well as larger platelets with mean diameters  $\pm$  SD of  $4.34 \pm 0.043$ ,  $3.88 \pm 0.045$  and  $2.61 \pm 0.025$   $\mu\text{m}$  from BSS-A, BSS-B and normal iPSCs, respectively ( $p < 0.001$ ). Overexpression of the GPIb in BSS-A-iPSCs using a lentiviral vector containing *GP1BA* gene improved proplatelet structures and decreased platelet sizes ( $3.184 \pm 0.078$   $\mu\text{m}$  [corrected BSS-A],  $4.453 \pm 0.096$   $\mu\text{m}$  [BSS-A],  $p < 0.001$ ) however the transgene was not expressed in BSS-B-iPSCs. Subsequently, IL-1 $\alpha$  and blebbistatin were used to explore BSS pathogenesis. The IL-1 $\alpha$ -induced MK rupture yielded larger platelets from normal iPSCs and there was no further increase in sizes of BSS-iPSCs-derived platelets. Furthermore, adding blebbistatin, a myosin II inhibitor, reduced the platelet sizes derived from BSS-iPSCs ( $3.20 \pm 0.035$  vs.  $4.38 \pm 0.046$   $\mu\text{m}$  [BSS-A],  $3.09 \pm 0.033$  vs.  $4.48 \pm 0.047$   $\mu\text{m}$  [BSS-B],  $p < 0.001$ ). Combining of blebbistatin and IL-1 decreased the mean sizes of BSS-iPSC-derived platelets ( $4.43 \pm 0.110$  vs.  $3.34 \pm 0.090$   $\mu\text{m}$  [BSS-A],  $4.60 \pm 0.103$  vs.  $3.20 \pm 0.089$   $\mu\text{m}$  [BSS-B]). Moreover, we constructed BSS-iPSC tubulin-GFP reporter lines which will be a useful tool for future studies of iPSC disease models. In conclusion, BSS-iPSCs could be used as a model for giant platelet disorders. Our data suggest that GPIb-IX-V is not necessary for IL-1 $\alpha$  induced platelet production, but likely involved in the proplatelet formation which is related to a myosin function.

Field of Study: Biomedical Sciences

Student's Signature .....

Academic Year: 2018

Advisor's Signature .....

## ACKNOWLEDGEMENTS

Firstly, I would like to express my sincere gratitude to my advisor Prof. Ponlapat Rojnuckarin for the continuous support of my Ph.D. study, for his patience, kindness, and invaluable advices. His guidance helped me in all the time of research and writing of this thesis. I could not have imagined having a better advisor for my Ph.D. study.

I also would like to express my honest thanks to Asst. Prof. Nipan Israsena who provided me an opportunity to join his team, and who allowed me to access the laboratory and research facilities. Without his precious supports it would not be possible to conduct this research. I also would like express my thanks to Dr. Ruttachuk Rungsviwat who first taught me the basic cell culture and iPS Cells and for his kindness as a RGJ senior.

Besides my advisor, I would like to thank the rest of my thesis committee: Asst. Prof. Tewin Tencomnao, Prof. Kanya Suphapeetipornand, Asst. Prof. Nipan Israsena and Prof. Pantep Anchaisuksiri for their insightful comments and encouragements and also for the precious suggestions which has been inspiring me to widen my idea of doing research.

I thank to CU stem cell lab members for their kindness for their help and for all the fun we have had in the last four years. In particularly, I also thank my friends Dr. Praewphan Ingrungruanglert for the stimulating discussions, problem solution and encouragement to me when I felt down. I also thank to Miss Netchanok Leela-adisorn for supporting to my lab work and she always spends time with me. I also thank Miss Sarinya Poadang for the great feeder cells and for the funny jokes that brought me smile. I also thank to hematology lab staffs for their help to collect patients' blood samples.

Finally, I would like to thank my dear family, my parents, my sisters and brothers for their supports, their love and understandings, which have brought me the today's success.

This study was supported by Thailand Research Fund (TRF), TRF through the Royal Golden Jubilee Ph.D. Program (Grant No. PHD/0120/2556) and the 100th Anniversary Chulalongkorn University Fund for Doctoral Scholarship.

Ponthip Mekchay

## TABLE OF CONTENTS

	<b>Page</b>
ABSTRACT (THAI) .....	iii
ABSTRACT (ENGLISH) .....	iv
ACKNOWLEDGEMENTS .....	v
TABLE OF CONTENTS .....	vi
LIST OF TABLES .....	ix
LIST OF FIGURES .....	x
CHAPTER I INTRODUCTION.....	1
1.1 Background and Rationale.....	1
1.2 Research Questions.....	2
1.3 Objectives of the study.....	2
1.4 Keywords.....	3
1.5 Conceptual Framework.....	3
1.6 Benefits and Applications.....	4
CHAPTER II LITERATURE REVIEW .....	5
2.1 Bernard-Soulier Syndrome .....	5
2.1.1 Signs and symptoms .....	5
2.1.2 Laboratory findings .....	5
2.1.3 Pathogenesis and pathophysiology.....	6
2.2 Glycoprotein Ib-IX-V Complex.....	6
2.3 Bernard Soulier syndrome in an animal model.....	9
2.4 Megakaryocytes, proplatelets formation and platelets biogenesis .....	10

2.5 Generation of platelets <i>in vitro</i> .....	12
2.6 Disease modeling and correction of platelet-related disease.....	14
CHAPTER III MATERIALS AND METHODS .....	16
3.1 Generation of induced pluripotent stem cells (iPSCs) from Bernard Soulier syndrome (BSS) patients.....	16
3.2 Induced pluripotent stem cell (iPSC) characterization.....	17
3.2.1 Reverse transcriptase Polymerase chain reaction (RT-PCR) for pluripotent stem cell marker expression.....	17
3.2.2 <i>In vitro</i> differentiation of the iPSCs line .....	18
3.2.3 Immunocytochemistry for pluripotent cell markers .....	19
3.2.4 Karyotyping.....	19
3.3 <i>In vitro</i> megakaryocyte and platelet differentiation via ES-Sacs method .....	19
3.4 Characterization of iPSC-derived hematopoietic progenitors, megakaryocytes (MKs) and platelets.....	20
3.4.1 Flow Cytometric Analysis.....	20
3.4.2 Immunocytochemistry.....	20
3.5 Genetic correction of BSS-iPSCs using lentiviral infection .....	21
3.6 Construction of iPSC lines with $\alpha$ -tubulin reporter .....	22
3.6.1 crRNA tubulin and donor vector design.....	22
3.6.2 Preparation of crRNA: tracrRNA duplex.....	22
3.6.3 Formation of the ribonucleoprotein (RNP) complex.....	22
3.6.4 Nucleofection .....	23
3.7 Testing the effects of pharmacological agents on platelet production .....	23
CHAPTER IV RESULTS .....	24



4.1 Generation of induced pluripotent stem cells (iPSCs) from Bernard Soulier syndrome (BSS) patients.....	24
4.2 Characterization of iPSCs .....	25
4.2.1 Pluripotent stem cell markers expression by reverse-transcriptase polymerase chain reaction (RT-PCR) .....	25
4.2.2 <i>In vitro</i> differentiation of the iPSC lines .....	26
4.2.3 Immunocytochemistry for pluripotent cell markers .....	28
4.2.4 Karyotyping.....	29
4.3 <i>In vitro</i> megakaryocyte and platelet differentiation via ES-Sacs method.....	29
4.4 Genetic correction of BSS iPSCs and platelet sizes .....	32
4.5 Construction of iPSC with tubulin 1B alpha GFP reporter lines .....	34
4.6 Pharmacological agent effects on platelet formation <i>in vitro</i> .....	35
CHAPTER V DISCUSSION .....	37
REFERENCES .....	40
VITA.....	46

## LIST OF TABLES

	Page
Table 1: Primers sets used for RT-PCR.....	18



## LIST OF FIGURES

	Page
Figure 1: GPIB-IX-V complex structure <sup>1</sup> .....	8
Figure 2: The two models of platelets generation; proplatelet formation and MKs rupture. <sup>23</sup> .....	11
Figure 3: Megakaryocytes and platelet differentiation via ES-SAC. <sup>42</sup> .....	14
Figure 4: iPSCs reprogramming from PBMCs of BSS patients, .....	25
Figure 5: RT-PCR analysis of stem cell marker genes in BSS-A-iPSCs, BSS-B-iPSCs and Normal iPSCs for expression of OCT4, NANOG, SOX2, c-MYC, KLF-4 and GAPDH. NC indicated negative controls. ....	26
Figure 6: In vitro differentiation of BSS-A and BSS-B iPSCs: Embryoid body (EB) formation on DAY 7, 14 and 21 of BSS-A (a.) and BSS-B (b.) .....	27
Figure 7: Immunofluorescence staining of endodermal (AFP), mesodermal (BRACHYURY) and ectodermal (NESTIN) markers of BSS-A (a.) and BSS-B (b.) embryoid bodies .....	27
Figure 8: Immunocytochemistry (ICC) staining for the pluripotency protein markers OCT4, and NANOG, SSEA4 and TRA-1-60 in BSS-A iPSCs (a.) and BSS-B iPSCs (b.).....	28
Figure 9: Metaphase karyotyping of BSS-A (a.) and BSS-B (b.).....	29
Figure 10: (a.) Upon ES-SAC differentiation, the sac-like structures were formed with hematopoietic progenitor cells (HPCs) inside (b.) On day 14 of differentiation, HPCs inside the sacs were harvested and stained for CD34. The normal, BSS-A and BSS-B iPSC-derived HPCs expressed CD34. ....	30
Figure 11: Megakaryocytes differentiation .....	31
Figure 12: Flow cytometry analysis of corrected BSS-A iPSC-derived MKs without (a.) and with doxycycline induced gene expression (b.) .....	33

Figure 13: Flow cytometry analysis of corrected BSS-B iPSC-derived MKs without (a.) and with doxycycline induced gene expression (b.) .....	33
Figure 14: Proplatelet formation (a.) and platelets size determination (b.) of corrected BSS-A iPSC- derived proplatelets without and with doxycycline induced GP1BA gene expression .....	34
Figure 15: Live cell images of iPSCs with tubulin-GFP: BSS-A iPSCs (Left) and BSS-B iPSCs (Right).....	35
Figure 16: Live cells images of BSS iPSC-derived HPCs on OP9 feeder cell on Day 15 of ES-SAC differentiation (Left) and BSS iPSC-derived proplatelet on day 21 of ES-SAC differentiation (Right).....	35
Figure 17: The determination of the mean sizes of iPSC-derived platelets from normal, BSS-A or BSS-B cultures (a.) In the absence or presence of IL-1 $\alpha$ and (b.) In the absence or presence of blebbistatin (c.) combined blebbistatin and IL-1 $\alpha$ condition .....	36

## CHAPTER I

### INTRODUCTION

#### 1.1 Background and Rationale

Bernard-Soulier Syndrome (BSS) is a severe bleeding disorder. Symptoms of BSS are variable depending on individuals but usually exhibit during early childhood. Clinical features of BSS patients are similar to other disorders of platelet dysfunction. These symptoms include mucocutaneous bleeding, gastrointestinal hemorrhage, purpuric skin bleeding and prolonged or heavy menstruation (menorrhagia) in female. Laboratory findings are characterized by prolonged bleeding time, low platelets count and presence of giant platelets on blood smears. Flow cytometry for Glycoprotein (GP) Ib/IX/V reveals a severe reduction or deficiency and platelet aggregation shows a failure of platelet to agglutinate when induced with ristocetin. <sup>1</sup>

BSS is an autosomal recessive macrothrombocytopenia caused by the defective in genes that encode for a group of linked proteins on platelets surface, GPIb-IX-V, a von Willebrand factor (VWF) receptor. They are composed of 4 genes (*GP1BA*, *GP1BB*, *GP9*, and *GP5*). Mutations of *GP1BA* are most commonly found in BSS, whereas mutations in *GP5* do not lead to BSS because *GP5* is not required for the expression of the complex but GPIb $\alpha$ , GPIb $\beta$ , and GPIX are gathered in the endoplasmic reticulum (ER) before exposure on platelet surface. The platelet GPIb-IX-V complex not only plays an important role in platelet activation but also plays a part of cytoskeletal binding via its C-terminal cytoplasmic tail to an actin filament network. Lacking of this complex on the cell surface results in large platelets. BSS Patients have normal numbers of megakaryocytes in the bone marrow, but have evidence of abnormal proplatelet formation and megakaryopoiesis. <sup>2</sup> The GPIb-IX-V complex may influence the late stage of megakaryopoiesis during the same time of platelet receptor expression. However, the mechanism of large platelet formation in this disorder is poorly understood.

Currently, there has been no available immortalized cell line that can produce platelet *in vitro*. There have been mouse models for megakaryocytes and platelet diseases. However, animal models are extremely expensive to generate, maintain and genetically modify. Furthermore, there are differences in mouse and human hematopoiesis and the findings in mice may not be all applicable to humans.

Nowadays, induced pluripotent stem cells (iPSCs) technology is an important tool to study in many research fields, such as diseases modelling, drug developing, drug screening and cell-replacement therapy in regenerative medicine. Induced pluripotent stem cells (iPSCs) are reprogrammed to an embryonic stem cell-like state by introducing genes important for maintaining the essential properties of embryonic stem cells (ESCs). The iPSC researches are now exploding in every sector of disease and academic part. We can use the patient sample-derived iPSCs to study the undefined disease pathogenesis *in vitro*. Therefore, in this study, we will use patient-specific iPSCs to understand the pathogenesis of BSS and explore for novel therapy.

### **1.2 Research Questions**

1. Do Bernard Soulier syndrome iPSC-derived megakaryocytes and platelets resemble megakaryocytes and platelets from Bernard Soulier syndrome patients?
2. Can the transgene rescue in Bernard Soulier syndrome iPSC restore the large platelet phenotype to normal phenotype?
3. Do cytoskeleton modifying agents affect sizes of BSS iPSC-derived platelets?

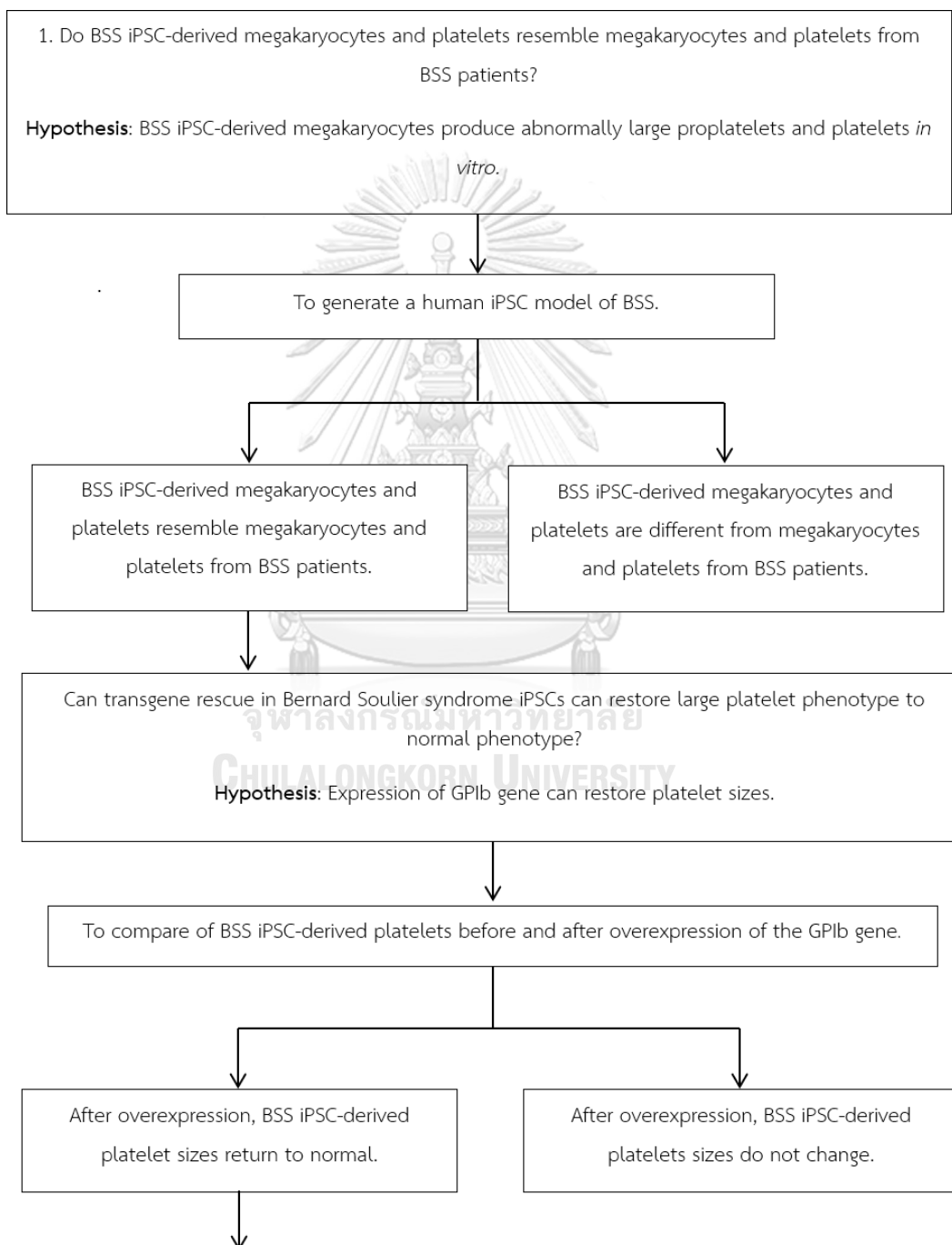
### **1.3 Objectives of the study**

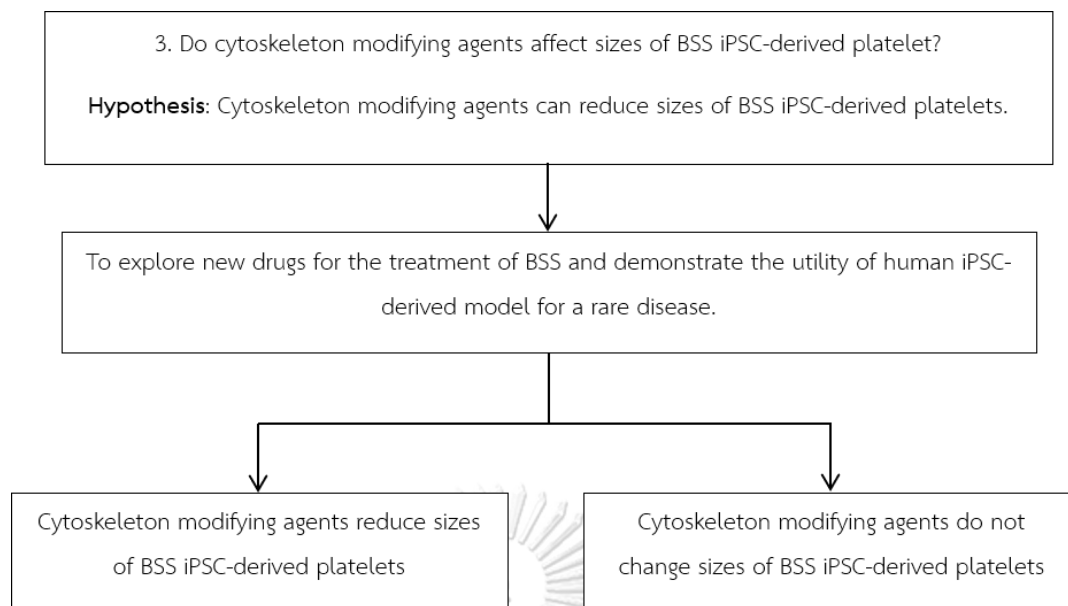
1. To generate a human iPSC model of Bernard-Soulier syndrome and demonstrate the utility of human iPSC-derived model for a rare disease.
2. To study of BSS iPSC-derived platelets before and after genetic correction.
3. To explore new drugs for the treatment of BSS using iPSC model

## 1.4 Keywords

Induced pluripotent stem cells (iPSCs), Bernard soulier syndrome, Megakaryocyte, Platelet, Macrothrombocytopenia

## 1.5 Conceptual Framework





### 1.6 Benefits and Applications

As the mechanisms of platelet production in health and diseases are still undefined, the iPSC technology can produce an important knowledge in various platelet diseases. The availability of patient-specific iPSC will yield the disease model to understand the pathogenesis of the disease. It is also used for drug screening and development. The gene correction may lead the way to autologous cell therapy for monogenic and acquired disease.



## CHAPTER II

### LITERATURE REVIEW

#### 2.1 Bernard-Soulier Syndrome

Bernard-Soulier syndrome (BSS) was first described by Dr. Jean Bernard and Dr. Jean Pierre Soulier in the year 1948. BSS is an inherited bleeding disorder that results in thrombocytopenia and platelet dysfunction. BSS is extremely rare. It has been estimated that this disease affects less than one person in a million based on case reports from Europe, North America, and Japan. However, misdiagnosis and under-reporting may affect this prevalence.<sup>3</sup>

##### 2.1.1 Signs and symptoms

BSS is characterized by the presence of the low platelets number with large sizes (macrothrombocytopenia). It is generally diagnosed in newborns or toddlers who experience unusual bleeding symptoms, such as epistaxis, ecchymosis, menorrhagia, gingival, gastrointestinal, muscular or visceral bleeding.<sup>3</sup> The clinical symptoms range from mild to severe. In severe cases, bleeding events can happen in surgical procedures or dental extractions or menstruations. Nonetheless, bleeding frequency and severity may differ among individuals.

##### 2.1.2 Laboratory findings

In BSS, the platelet counts can vary from mildly decreased to normal, usually ranges from less than 80 to 100 × 10<sup>3</sup>/μL. The peripheral blood smear shows large platelets. Bleeding time is prolonged.<sup>4</sup> The diagnosis can be confirmed by platelet aggregation studies, flow cytometry and gene sequencing. By platelet aggregation, BSS platelets will aggregate in response to epinephrine, collagen and ADP but they will not aggregate in the presence of ristocetin.<sup>1</sup> This failure to agglutinate cannot be corrected by the addition of normal plasma, therefore, we can discriminate BSS from von Willebrand disease (VWD). Meanwhile, flow cytometric analysis of platelets is also characteristic for BSS showing normal binding to CD41 (GP IIb) and CD61 (GPIIIa) antibodies, but defective binding to CD42a (GPIX), CD42b (GP Ib $\alpha$ ), CD42c (GP Ib $\beta$ ), and

CD42d (GPV) antibodies. Furthermore, for *GP1BA*, *GP1BB*, and *GP9* gene sequencing, including coding and noncoding regions, is necessary to confirm the platelet receptor gene mutations.

### 2.1.3 Pathogenesis and pathophysiology

Bernard-Soulier syndrome is an autosomal recessive disorder, in which platelet surface GPIb-IX-V complex is decreased or absent. These platelet glycoprotein complex acts as a binding site for von Willebrand factor (VWF), which is necessary for platelet aggregation by linking between platelet and sub-endothelial extracellular matrix collagen fibrils at sites of injury. This interaction between the GPIb-IX-V complex, VWF and collagen is crucial for platelet adhesion and subsequent platelet aggregation. Losing of this protein complex will affect platelets plug formation causing bleeding tendency. BSS mutations may be classified based on a biosynthesis defect or functional defect.<sup>5</sup> Mutations of GPIb $\alpha$ , GPIb $\beta$  and GPIX genes result in BSS type A, type B and type C, respectively.

## 2.2 Glycoprotein Ib-IX-V Complex

The glycoprotein (GP) Ib-IX-V complex is a crucial platelet receptor in initiating and propagating hemostasis. It was first discovered in 1948.

### Structure and functions

The GPIb-IX-V complex is a primary platelet adhesion receptor that consists of four distinct transmembrane proteins, GPIb $\alpha$  (MW 135 kDa), GPIb $\beta$  (MW 26 kDa), GPIX (MW 20 kDa) and GPV (MW 82 kDa), creating the functional receptor on the surface of megakaryocytes. The four subunits are separately encoded by 4 genes mapping to chromosomes 17p12 (*GP1BA*), 22q11.2 (*GP1BB*), 3q29 (*GP5*) and 3q21 (*GP9*). The four genes belong to the leucine-rich family of proteins and are exclusively expressed in platelets under physiological conditions. They have a simple structure with the coding sequence contained within a single exon, except for *GP1BB* which contains an intron of 10 bases after the start codon. The GPIb $\alpha$  form disulfide links to two GPIb $\beta$  subunits,

GPV and GPIX proteins at a ratio of 2:4:2:1.<sup>1</sup> (**Figure 1**) The surface expression of the whole complex needs GPIb $\alpha$ , GPIb $\beta$ , and GPIX. Lack of a single subunit will affect receptor synthesis except for GPV which is not necessary for receptor expression, or vWF binding function. Knocking out the GPV in mice has no effect on megakaryocyte (MK) ultrastructure, platelet production, size or GPIb-IX expression.

In the GPIb-IX-V complex, the main ligand-binding subunit is located in the GPIb $\alpha$ . The adhesive ligands, including von Willebrand factor (VWF), thrombospondin, counter receptors on endothelial cells (P-selectin) or leukocytes (integrin $\alpha_M\beta_2$ ), and coagulation factors (thrombin, factors XI and XII, high-molecular-weight kininogen), bind to the N-terminal ligand-binding region (His1-Glu-282).

The cytoplasmic domain of GPIb-IX-V interacts with multiple intracellular binding partners, controlling platelet size/shape and/or signal transduction. The interaction of GPIb-IX-V and filamin A, the cytoskeletal protein, has been reported to control platelet size, shape change and adhesive function through a binding site involving Phe568/Trp570 within the GPIb $\alpha$  cytoplasmic tail.<sup>6</sup> In megakaryocytes, filamin A controls normal platelet production and normal GPIb $\alpha$  expression on circulating platelets.<sup>7</sup> Disruption of the link between cytoplasmic tail of GPIb $\alpha$  and components of platelet membrane cytoskeleton may result in platelet size abnormalities. As part of signaling transduction, human GPIb-IX-V interacts with structural signaling proteins, such as calmodulin, 14-3-3 $\zeta$  and the p85 subunit of phosphoinositide 3-kinase.

Engagement of GPIb $\alpha$  by the VWF A1-domain initiates intracellular signaling leading to inside-out activation of the platelet integrin,  $\alpha_{IIb}\beta_3$  (GPIIb-IIIa) that binds fibrinogen or VWF and mediates platelet aggregation and clot contraction. GPIb $\alpha$  also binds to the integrin,  $\alpha_M\beta_2$  (CD11b/CD18; Mac-1) on activated leukocytes in inflammatory responses.<sup>8</sup> In experimental models, GPIb $\alpha$  has been shown to regulate venous, as well as arterial thrombus formation at lower or higher shear rates. In addition to binding the VWF A1-domain, the regulation of thrombus formation may possibly also be from interactions with coagulation factors (thrombin and factors XII/XI)



### 2.3 Bernard Soulier syndrome in an animal model

BSS animal model has been reported in various studies. Ware *et al.*, demonstrated that murine model exhibited the BSS-like phenotype (macrothrombocytopenia or giant platelets) after disruption of the  $\alpha$ -subunit of gene encoding for GPIb-IX-V complex. Human GPIb $\alpha$  expression by transgenic technology could restore the BSS mouse platelets to the normal size. However, platelets count was not restored to the normal level when compared with wildtype.<sup>9</sup> Furthermore, megakaryopoiesis studies in mouse deficient of GPIb $\beta$  exhibited some normal megakaryocytes properties (number, differentiation, endoreplications) in bone marrow but showed abnormal structure of thick peripheral zone and poor developed demarcation membrane system. Mature megakaryocytes displayed abnormal morphology of proplatelets which have fewer branches and thicker shafts. Besides that, platelets sizes were abnormally large with thick tubulin rings.<sup>10</sup>

Gene therapy of BSS has been examined using lentiviral vector (LV). For example, S. Kanaji *et al.*<sup>11</sup> introduced human *GP1BA* under control of the platelet-specific integrin  $\alpha$ IIb promoter (2bIb $\alpha$ ). Lentiviral vectors containing human *GP1BA* were transduced into hematopoietic stem cells (HSC) of GPIb $\alpha$  null mouse and transplanted into bone marrow after transplantation. The mouse cells could synthesize transgene protein, human GPIb $\alpha$  (hGPIb $\alpha$ ), which was able to form the complex with mouse proteins GPIb $\beta$  and IX and the macrothrombocytopenia and bleeding phenotype in BSS mice were rescued.<sup>11</sup> Meanwhile the role of GPIb $\beta$  was studied in a Bernard–Soulier mouse model lacking GPIb $\beta$  subunit by transduced viral particles harboring human GPIb $\beta$  (hGPIb $\beta$ ) into GPIb $\beta$ <sup>null</sup> Sca-1<sup>+</sup> progenitors and transplanted into lethally irradiated GPIb $\beta$ <sup>null</sup> mice bone marrow. The hGPIb $\beta$  transplanted mice showed 97% rescued of GPIb-IX expression in circulating platelets. This model also demonstrated the crucial role of GPIb $\beta$  intracellular domain in GPIb-IX expression. For instance, the removal of the GPIb $\beta$  membrane proximal segment (D150-160) resulted in decreasing of GPIb-IX expression leading to increased bleeding time and decreased thrombotic tendency.<sup>12</sup>

Although BSS animal models can represent the phenotypes of BSS, there are some limitations of the use of mouse models as they do not reproduce all aspects of

human disease conditions. Mice have small size bodies, short life-spans and the disease progression which are different from humans.<sup>13</sup>

## **2.4 Megakaryocytes, proplatelets formation and platelets biogenesis**

Platelets are the smallest anucleated cell fragments flowing in the blood circulating system. The platelet diameter ranges from 1-3  $\mu\text{m}$ .<sup>14</sup> Platelets are involved in many processes, such as hemostasis, wound healing, angiogenesis, inflammation, and innate immunity. Platelets are produced from cytoplasm of megakaryocytes (MKs) inside bone marrow.<sup>15</sup> MKs are developed from hematopoietic stem cells (HSCs) that reside mainly in the bone marrow.<sup>14</sup> MKs are rare cell population which represents approximately 0.01% of total cells in bone marrow. The size of MKs is approximately 50–100  $\mu\text{m}$ .<sup>16</sup>

Platelet formation composed of two steps. The first step is MK maturation and development which requires MK-specific growth factors. Thrombopoietin (TPO) is the major cytokine promoting MK development from HSC precursors and control of endomitosis causing mononuclear MK to become polyploid.<sup>17</sup> Nuclear proliferation and enlargement of the MK cytoplasm occurs as MKs are filled with cytoskeletal proteins, platelet-specific granules, and sufficient membrane to complete the platelet assembly process. The second phase is relatively rapid and can be completed within hours. During this phase, MKs generate platelets by remodeling their cytoplasm firstly into proplatelets and then into preplatelets, which undergo subsequent fission events to generate discoid platelets. The time that used all process is approximately 5 days from MKs to complete polyploidization, mature and platelet releases.<sup>14,18-20</sup> The crucial factors, which are related to platelets sizes, are proplatelet formation and <sup>21</sup>platelet cytoskeleton proteins. Up to date, the platelet production can be classified into 2 pathways. Firstly, the classic mechanism of proplatelets formation occurred from TPO drives of megakaryopoiesis. MK cytoplasm then produces long protrusion (proplatelets) extending into bone marrow sinusoid and then fragmented into platelets. Platelets released from this pathway have normal sizes. The goal of this pathway is to maintain platelets number in blood circulation at a steady state. Second pathway is megakaryocytes rupture which occurs in conditions with acute platelet needs, such as

inflammations, infection, immune thrombocytopenia and traumatic blood loss. This MK rupture produces larger platelet numbers, more than 20-fold compared to classic pathway.<sup>22</sup> MKs rupture is induced by interleukin-1 $\alpha$  (IL-1 $\alpha$ ) which is released from injured endothelium or activated platelets (Rider et al., 2013) IL-1 $\alpha$  signaling activates Caspase-3 pathway resulting in MK losing membrane stability and leading to membrane blebbing together with deregulation and organization of  $\beta$ 1-tubulin. This process causes larger platelet sizes with normal function.<sup>23</sup>

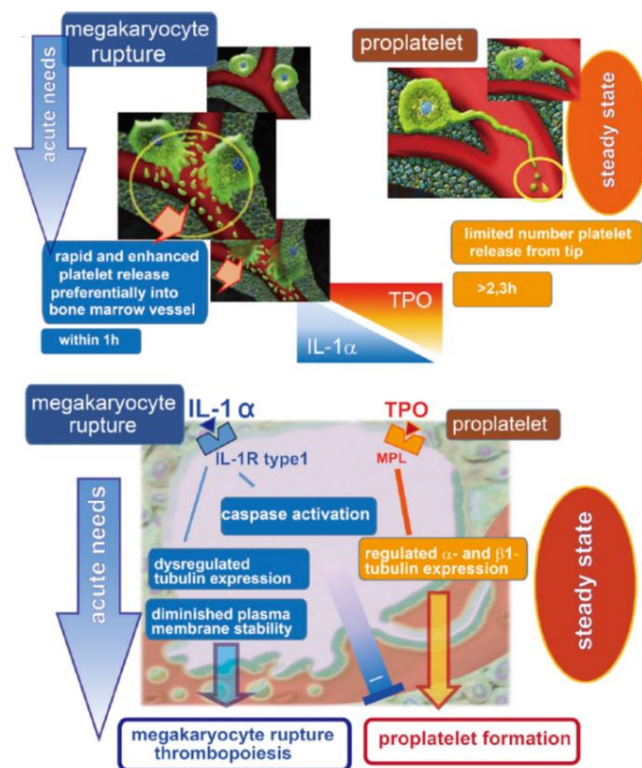


**Figure 2:** The two models of platelets generation; proplatelet formation and MKs rupture.<sup>23</sup>

Once platelets are released into the bloodstream, they survive 7–10 days.<sup>24-26</sup> The production of platelets by megakaryocytes requires an intricate series of remodeling events that result in the release of thousands of platelets from a single megakaryocyte. Abnormalities in this process can result in clinically significant disorders. Megakaryocytes cytoskeletal reorganization is the risky phase in platelets production which is regulated by the major cytoskeleton proteins, tubulin and actin.

Microtubule is involved in proplatelet extension and elongation process by the polymerization of  $\beta$ 1 and  $\alpha$ -tubulin.<sup>27</sup> The thickness and the diameter of microtubule coil at the end of proplatelet are related to platelet size and its discoid shape.<sup>28</sup> Furthermore the microtubules cytoskeleton interacts with actin filaments. Actin regulates proplatelet shaft bending and branching to increase the number of proplatelet ends and platelet releases. In addition, actin-modulating proteins, such as filamin and myosin may affect cytoskeletal remodeling and may regulate platelet sizes.<sup>28</sup> For example, myosin is an actomyosin filament/plasma membrane cross-linker molecule which is necessary cytoskeleton protein for platelets shape change.<sup>29-32</sup> Blebbistatin, a myosin II inhibitor, affects MK membrane fragmentation from large to normal sizes of pre-/pro-platelets. Myosin has been reported to destabilize microtubule marginal bands that maintain resting platelet discoid shape<sup>33</sup> via contraction of actomyosin structures.<sup>4</sup>

In BSS, MK numbers in bone marrow are shown to be normal suggesting that the cause of macrothrombocytopenia occurs in the final stages of platelet production. MKs from BSS exhibit thicker peripheral microtubules, large proplatelet tip production and vacuolated invaginated membrane systems. BBS platelets are associated with abundant cytoplasmic vacuoles and abnormal concentration of membrane complex in discrete zones. Understanding the molecular pathogenesis of these abnormalities will give us deeper insights in the mechanisms of both abnormal and normal platelet production.

## 2.5 Generation of platelets *in vitro*

Platelets are the progeny of megakaryocytes, a rare population of hyperploid cells that reside in the adult bone marrow. Platelets are generated by the extension of pro-platelet-like structures into the vasculature. These extensions shed thousands of cell fragments into the circulation under shear forces of blood flow.<sup>34,35</sup> The formation of MKs and platelets requires specific transcription factors, including GATA-1, NF-E2, and SCL, which also play key roles in erythropoiesis.<sup>36,37</sup> In addition, megakaryocyte numbers, maturation, and pro-platelet formation are dependent on the growth factor, thrombopoietin (TPO)<sup>38,39</sup>



The first study of mature megakaryocytes generation from hESCs was reported by Gaur et al.<sup>39</sup> in 2006. The hESCs were differentiated on OP9 feeder cells which supported the hematopoietic cell differentiation of mouse and human ESCs *in vitro*. After 15–17 days of co-culture supplemented with TPO, these cells expressed MK-specific surface antigens, including the lineage markers CD41a (integrin  $\alpha$ IIb or GPIIb) and CD42b (GPIb $\alpha$ ) in the ESC-derived megakaryocytes. Anyway, no platelets could be detected.<sup>39</sup> After that, Takayama et al.<sup>21</sup> revised Gaur et al.<sup>39</sup> protocol by co-culturing ESCs on either OP9 or C3H10T1/2 stroma for 14–15 days of differentiation and induced with vascular endothelial growth factor (VEGF) which led to sac-like structures (ES-sacs) formation. ES-sacs are consisted of a morphologically distinct outer layer of cells with endothelial-like properties and a population of round hematopoietic-like cells expressing shared markers of blood and endothelium, such as VE-cadherin and CD31, as well as the hematopoietic cell-specific markers CD34, CD41a, and CD45.<sup>21</sup> These hematopoietic cells have the capacity to form hematopoietic colonies *in vitro*. When cultured for 24 days in medium that was supplemented with VEGF and TPO plus other cytokines (interleukin [IL]-6, IL-11, and stem cell factor [SCF]), the hematopoietic progenitors from ESC sacs formed megakaryocytes. In addition, megakaryocytes obtained in this manner released platelets that expressed CD41a and CD61 (integrin  $\beta$ 3 or GPIIIa) and could be activated in response to ADP and thrombin. However, hESC-derived megakaryocytes contained fewer granules and yielded far fewer platelets *in vitro* than their normal counterparts *in vivo* (2–3 compared with  $\sim$ 1,000-3,000 platelets per megakaryocyte).<sup>21,40</sup> In addition, the *in vivo* functions of the ES sac-derived platelets have not been demonstrated.

In 2010 the generation of hiPSC-derived megakaryocytes and platelets with *in vivo* functions by using hiPSCs derived from human dermal fibroblasts, instead of hESCs, was reported.<sup>41</sup> The platelet yield per megakaryocyte under these conditions was improved by approximately two- to threefold, compared with their previous study. The hiPSC-derived platelets were detectable in the circulation for at least 24 hours after transfusion into irradiated NOD-SCID-*Il2rg*<sup>-/-</sup> mice by using intravital microscopy to observe the transfused platelets participating in the formation of blood clots after laser-induced vessel injury.

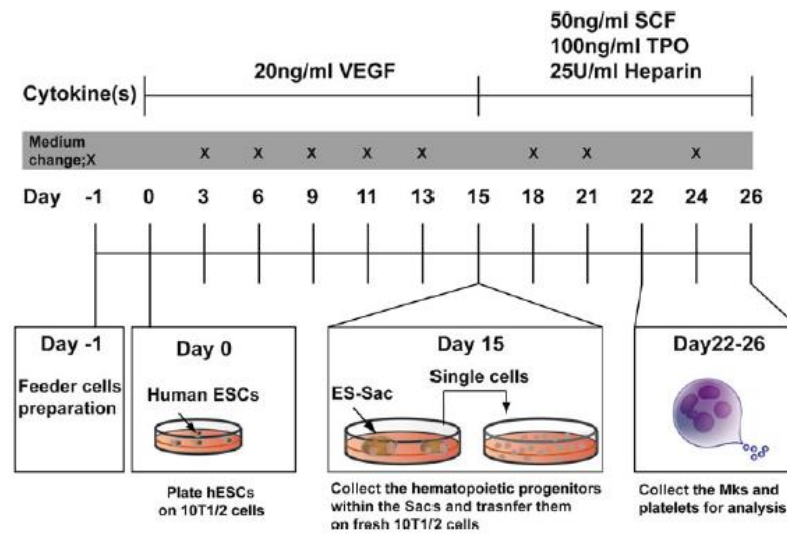


**Figure 3:** Megakaryocytes and platelet differentiation via ES-SAC. <sup>42</sup>

## 2.6 Disease modeling and correction of platelet-related disease

As megakaryocytes (MKs) and platelets can be generated from human ESCs and iPSCs in vitro, this is a potential source of blood cells for clinical transfusion and a promising tool for studying the human thrombopoiesis. Moreover, disease-specific iPSCs are powerful models for elucidating the pathogenesis of hematological diseases and for drug screening.

Disease modeling and gene correction of Glanzmann thrombasthenia, congenital amegakaryocytic thrombocytopenia (CAMT) and Wiskott-Aldrich syndrome (WAS) were recently reported. <sup>43 44</sup> CAMT is a disorder caused by mutations in the C-mpl gene that lead to loss of TPO/MPL signaling. This disorder is phenotypically with severe aberrant hematopoiesis and fatal prognosis. <sup>45</sup> Due to the lack of primary cells, it is extremely challenging to study bone marrow-derived progenitors for a greater insight into the mechanism of action and potential targets of drug therapy. The CAMT patient-derived iPSCs were created from the dermal fibroblasts. <sup>43</sup> These cells displayed a characteristic inability to differentiate toward the megakaryocyte lineage. This defect was attributed, in part, to dysregulated expression of FLI1, a megakaryocyte specific transcription factor. Importantly, C-mpl retroviral delivery was sufficient to restore megakaryocyte lineage specification of CAMT iPSCs.

Besides that, mononuclear cells from the peripheral blood of two patients with Glanzmann thrombasthenia were re-programmed into iPSCs and subsequently corrected by gene therapy.<sup>44</sup> Glanzmann thrombasthenia is caused by mutations in integrin  $\alpha_{IIb}\beta_3$  leading to a platelet aggregation defect and can cause severe bleeding. The corrected  $\alpha_{IIb}$  cDNA was inserted into the 'safe harbor' AAVS1 locus to minimize potential endogenous activation and was driven by the GPIb $\alpha$  promoter for megakaryocyte-specific expression. Megakaryocyte differentiated from the corrected cell lines were stained positive for the PAC-1 antibody when treated with platelet agonists, suggesting that  $\alpha_{IIb}\beta_3$  was present on the cell surface and inducible to an activated state. This study is an important first step to elucidate the efficacy of gene correction for Glanzmann thrombasthenia in an effort to create iPSC-derived material for syngeneic transplant.

There is a recent study of a model for Wiskott-Aldrich syndrome (WAS), an X-linked recessive disorder with mutations in WAS protein (WASP) gene, a regulator of actin cytoskeleton and chromatin structure in various blood cell lineages. The patients present with microthrombocytopenia, complex immunodeficiency, autoimmunity, and propensity for hematologic malignancies. Generation of induced pluripotent stem cell (iPSC) from WAS patients exhibited defects in platelet production *in vitro*. WAS-iPSCs produced platelets with irregular shapes and smaller sizes. In addition, abnormal cytoskeletal rearrangement, F-actin distribution, and proplatelet formation were observed under immunofluorescence and electron microscopy. Overexpression of WASP in the WAS-iPSCs using a lentiviral vector improved proplatelet structures and normalized the platelet sizes.<sup>46</sup>

Finally, a study of megakaryopoiesis using the iPSCs model of BSS will identify a requirement of GPIb-IX-V in proplatelet formation and platelet production with normal size and shape. This study will provide a good indication that patient-derived iPSCs model properly recapitulate defects in a human disease and the use of this model will give knowledge of the mechanisms of megakaryocyte maturation and platelet formation in order to improve diagnosis and investigate for new treatments in the future.

## CHAPTER III

### MATERIALS AND METHODS

#### 3.1 Generation of induced pluripotent stem cells (iPSCs) from Bernard Soulier syndrome (BSS) patients

Following the iPSCs reprogramming protocol from Center for iPS Cells Research and Application at Kyoto University (CiRA), whole blood samples were obtained from BSS patients. Peripheral blood mononuclear cells (PBMCs) were separated from whole blood by using Ficoll®-Paque Premium (GE Healthcare, Sweden) and gradient centrifugation. After centrifugation, the PBMC layer was removed from the tube and transferred to a new tube. PBMCs were washed with 1X PBS, resuspended in 5 ml of PBMCs culture medium (StemSpan H3000, StemCell Technologies, USA) and then counted for the number of cells. Extra PBMCs could be frozen down. PBMCs were cultured at  $2-4 \times 10^6$  cells/ml by adding 2 ml to each well of a non-TC treated 6-well plate. 1.5 ml of PBMC culture medium was added into each well every 2–3 days. Cells were cultured at 37 °C for 7–8 days in a CO<sub>2</sub> incubator with a water tray to maintain the humidity.

On the day of nucleofection, cells were harvested and counted for the number. The reprogramming method is by Lonza 4-D Nucleofector™ System using PBMCs  $1 \times 10^6$  cells/vial. The episomal vector stock solution was prepared by premixing the four vectors, pCXLE-hOct3/4-shp53-F plasmid (Addgene plasmid # 27077; <http://n2t.net/addgene:27077>; RRID:Addgene\_27077), pCXLE-hSK plasmid (Addgene plasmid # 27078; <http://n2t.net/addgene:27078>; RRID:Addgene\_27078), pCXLE-hUL plasmid (Addgene plasmid # 27080 ; <http://n2t.net/addgene:27080> ; RRID:Addgene\_27080) and pCXWB-EBNA1 plasmid (Addgene plasmid # 37624 ; <http://n2t.net/addgene:37624> ; RRID:Addgene\_37624) for expression of OCT3/4, SOX2, KLF4 and L-MYC, in equimolar amounts and set up a stock concentration of 0.83 µg for each plasmid. (Total stock concentration of plasmids would be 0.6 µg/µL). The nucleofection solution (Amaxa CD34<sup>+</sup> cell Nucleofector Kit, Lonza, Germany) was

added to suspended cells. After that, nucleofection was performed using program CD34 reprogramming. The cells were then plated onto MEF feeder cells in a 6 cm plate with PBMC culture medium. On day 8, 10 and 12 the 1.5 ml of mTeSR™1 medium (StemCell Technologies, USA.) was added and replaced on day 14, 17, 20, 23. On day 25 to 35, colonies of approximately 2 mm diameter were picked.

### 3.2 Induced pluripotent stem cell (iPSC) characterization

#### 3.2.1 Reverse transcriptase Polymerase chain reaction (RT-PCR) for pluripotent stem cell marker expression

Total RNA from undifferentiated BSS-iPSC lines and a control iPSC line were isolated using TRI Reagent® RNA isolation reagent (Molecular Research Center, Inc., USA.). The cDNA from total mRNA was synthesized using RevertAid™ H Minus M-MuLV (Fermentas, Glen Burnie, MD, USA) for RT-PCR. Endogenous pluripotency-associated transcription factors *SOX2*, *NANOG*, *cMYC*, *KLF4*, *OCT4* and house-keeping *GAPDH* genes were amplified using CloneAmp HiFi PCR (Takara Bio Inc., China). PCR products were visualized in 1% agarose gel. The separate primer sets for *SOX2*, *NANOG*, *cMYC*, *KLF4*, *OCT4* and *GAPDH* were used to confirm the expression of pluripotent markers Primers used are shown in **Table 1**.

**Table 1:** Primers sets used for RT-PCR.

Gene	Primer Sequence	Product Size (bp)	Reference
<i>GAPDH</i>	Forward: AAC AGC CTC AAG ATC ATC AGC Reverse: TTG GCA GGT TTT TCT AGA CGG	338	Takayama et al <sup>21</sup>
<i>OCT4</i>	Forward: GAA GGT ATT CAG CCA AAC GC Reverse: GTT ACA GAA CCA CAC TCG GA	313	Lu et al <sup>47</sup>
<i>NANOG</i>	Forward: ATA CCT CAG CCT CCA GCA GA Reverse: CAG GAC TGG ATG TTC TGG GT	391	Takahashi et al <sup>48</sup>
<i>SOX2</i>	Forward: GGG AAA TGG GAG GGG TGC AAA AGA GG Reverse: TTG CGT GAG TGT GGA TGG GAT TGG TG	151	Takahashi et al <sup>48</sup>
<i>cMYC</i>	Forward: GCG TCC TGG GAA GGG AGA TCC GGA GC Reverse: TTG AGG GGC ATC GCT GCG GGA GGC TG	328	Takahashi et al <sup>43</sup>
<i>KLF4</i>	Forward: TGA TTG TAG TGC TTT CTG GCT GGG CTC C Reverse: ACG ATC GTG GCC CCG GAA AAG GAC C	397	Takahashi et al <sup>48</sup>

### 3.2.2 *In vitro* differentiation of the iPSCs line

The *in vitro* pluripotent capacity of the BSS iPSC cell lines were tested by spontaneous embryoid body (EB) differentiation. One ml of Matrigel (CORNING, USA.) was added to the culture plate one to two days before iPSC reaching confluence. The eighty percent confluent iPSCs were washed with 1 ml of 1XPBS and incubated with 0.5 ml of CTK solution consisting of 0.25% trypsin (Thermo Fisher Scientific., USA.), 0.1% collagenase IV (Thermo Fisher Scientific., USA), 20% Knockout serum replacement (KSR; Thermo Fisher Scientific, USA) and 1 mM CaCl<sub>2</sub> in dH<sub>2</sub>O for 5-7 min. CTK was aspirated and iPSC colonies were washed with 1XPBS for 2 times. The iPSCs were resuspended to the clumps and cultured in ultra-low attachment wells (Sigma-Aldrich) to induce EB formation. EBs were cultured for 21 days with EB medium consisting of DMEM/F12 (Hyclone, GE Healthcare Lifesciences, USA) supplemented with 20% FBS (Thermo Fisher Scientific, USA), 1% nonessential amino acids (Thermo Fisher Scientific, USA), 0.1 mM  $\beta$ -mercaptoethanol (Thermo Fisher Scientific, USA), and 1% Antibiotic-Antimycotic

(Thermo Fisher Scientific, USA) without basic fibroblast growth factor 2 (bFGF2) for spontaneous differentiation to the three germ layers. Medium changes were performed every 2–3 days. Immunocytochemistry was used to analyze the germ layer associated markers: Nestin (BioLegend) for ectoderm, Brachyury (Abcam) for mesoderm and AFP (Abcam) for endoderm at the end of differentiation.

### 3.2.3 Immunocytochemistry for pluripotent cell markers

BSS iPSCs were fixed with 4 % paraformaldehyde for 15 minutes at room temperature and then permeabilized with 1XPBS supplemented with 0.3 % Triton X-100 for 15 min. BSS iPSCs were then blocked in blocking solution (10 % goat serum and 0.3 % Triton X-100 in PBS) for 30 minutes at room temperature and stained with primary antibodies to Oct4 (Cell Signaling technology<sup>®</sup>), Nanog (Cell Signaling technology<sup>®</sup>), Tra-1–60 (Cell Signaling technology<sup>®</sup>), and SSEA-4 (Abcam) at 4°C overnight. Cells were then stained with the Alexa Fluor conjugated secondary antibody (Molecular Probes, Invitrogen) for 1 hour.

### 3.2.4 Karyotyping

Chromosomal analysis of every iPSC line was performed by the Chromosome Laboratory Center, Bangkok, Thailand.

## 3.3 *In vitro* megakaryocyte and platelet differentiation via ES-Sacs method

The BSS-iPSCs were co-cultured on C3H10T1/2 feeder cells in the presence of vascular endothelial growth factor (VEGF) for 14 days. On the day 14 of differentiation, ES-sacs were torn by needles then cells were collected and passed-through a 40 µm cell strainer. Subsequently, hematopoietic progenitors from ES-sacs were transferred to feeder cells and cultures in megakaryocytes differentiating medium in the presence of 100 ng/ml human thrombopoietin (TPO; R&D Systems), 50 ng/ml human stem cell factor (SCF; R&D Systems) and 25 U/ml heparin (Sigma-Aldrich, St Louis, MO, USA). On day 21, the non-adherent cells were collected and analyzed.

### 3.4 Characterization of iPSC-derived hematopoietic progenitors, megakaryocytes (MKs) and platelets

#### 3.4.1 Flow Cytometric Analysis

Flow Cytometric Analysis of the surface molecules of progenitor cells separated from ES-sacs were stained with APC-conjugated anti-human CD34 (BD Biosciences, San Jose, CA, USA) and PerCP-conjugated anti-human CD45 (BD Biosciences) for hematopoietic progenitor cell analysis on day 14 of differentiation.

FITC-conjugated anti-human CD41a (BioLegend) and PE-conjugated anti-human CD42b (BioLegend) were used to detect megakaryocyte differentiation on day 21 of differentiation and platelet-like particles on day 23 of differentiation. BD FACS Aria II (Becton Dickinson, Franklin Lakes, NJ, USA) was used to analyze. For platelet analysis, platelet-like particles in culture supernatant were gated using the same FSC and SSC as normal platelets.

#### 3.4.2 Immunocytochemistry

For platelet staining, platelet-containing supernatant containing 1  $\mu\text{M}$  prostaglandin E1 was centrifuged at 2,000 rpm. Platelet pellets were resuspended and smeared onto the matrigel-coated coverslips and dried.

For proplatelet staining, iPSC-derived megakaryocytes on day 21 of culture were reseeded onto matrigel-coated coverslips and cultured for 24 hours. Subsequently, they were fixed with 4 % formaldehyde for 15 min at room temperature and permeabilized with 1XPBS supplemented with 0.3 % Triton X-100 for 15 min. Proplatelets and platelets were then blocked in the blocking solution for 30 min at room temperature and stained with anti- $\alpha$ -tubulin (Abcam, Cambridge, MA, USA) and phalloidin-FITC. (Molecular Probes, Invitrogen., USA.) One  $\mu\text{g}/\text{ml}$  DAPI (Molecular Probes, Invitrogen, USA) was used for nuclear staining. All fluorescence images were obtained using Axio Observer fluorescent microscopy (Carl Zeiss, Jena, Germany). The shortest diameters of tubulin-stained discoid-shaped platelets were measured using AxioVision Rel 4.8 (Carl Zeiss).



### 3.5 Genetic correction of BSS-iPSCs using lentiviral infection

*GP1BA* or *GP1BB* cDNA was amplified and cloned into plvx-TRE3G vector using In-Fusion HD (Takara Bio Inc., USA.). Vectors containing *GP1BA* or *GP1BB* were combined with Lenti-X-packaging single shot (VSV-G) and co-transfected into Lenti-X 293T cell line. Two days after transfection, the media were collected and filtered through a 0.45  $\mu\text{m}$  pore size filter. Harvested lentiviral supernatant was centrifuged at 25,000 rpm for 90 minutes to concentrate viral particles. Viral pellets were resuspended with Opti-MEM (Invitrogen, USA.).

BSS-A-iPSCs were, supplemented with 6  $\mu\text{g}/\text{ml}$  polybrene, infected by viral pellets containing plvx-TRE3G-*GP1BA* and plvx-EF1a-Tet3G. BSS-B-iPSCs were, supplemented with 6  $\mu\text{g}/\text{ml}$  polybrene, infected by viral pellets containing plvx-TRE3G-*GP1BB* and plvx-EF1a-Tet3G for 8-24 hour. BSS-A-iPSCs and BSS-B-iPSCs containing *GP1BA* and *GP1BB* gene clones, respectively, were selected by using puromycin (Gibco™, Fisher Scientific, China) 0.5  $\mu\text{g}/\text{ml}$  and geneticin (Gibco™, Fisher Scientific., Thailand) 80  $\mu\text{g}/\text{ml}$ . They were then expanded and screened for doxycycline-inducible expression.

For GPIb overexpression experiment, proplatelets and platelets were stained with anti- $\alpha$ -tubulin (Abcam) and phalloidin-FITC. After that, cells were fixed, permeabilized and blocked. One  $\mu\text{g}/\text{ml}$  DAPI (Molecular Probes, Invitrogen) was used for nuclear staining. All fluorescence images were obtained using Axio Observer fluorescence microscopy (Carl Zeiss, Jena, Germany). The shortest diameters of tubulin-stained discoid-shaped platelets were measured by using AxioVision Rel 4.8 (Carl Zeiss).

### 3.6 Construction of iPSC lines with $\alpha$ -tubulin reporter

#### 3.6.1 crRNA tubulin and donor vector design

The crRNA tubulin was designed based on donor vector homology arm, which was described by Roberts et al<sup>49</sup>, using Custom Alt-R<sup>®</sup> CRISPR-Cas9 guide RNA design tool (IDT). Designed crRNA sequence was shown below.

***TUBA1B* crRNA 5'-GATGCACTCACGCTGCGGGA -3'**

All CRISPR/CAS9 system was obtained from Stem Cell and Cell Therapy Research Unit, Faculty of Medicine, Chulalongkorn University, Bangkok, Thailand. The commercially-produced gRNA was used to ensure quality and consistency across the editing experiments. (IDT, USA)

Donor vector; AICSDP-4: *TUBA1B*-mEGFP (Addgene plasmid # 87421; <http://n2t.net/addgene:87421>; RRID: Addgene\_87421) which has been used with locus-specific CRISPR/Cas9 to add a mEGFP tag to the second exon of human *TUBA1B* in WTC human induced pluripotent stem cells by the Allen Institute for Cell Science was used in this study.<sup>49</sup>

#### 3.6.2 Preparation of crRNA: tracrRNA duplex

Each RNA oligonucleotide (Alt-R CRISPR-Cas9 tubulin crRNA and Alt-R CRISPR-Cas9 tracrRNA) was resuspended in Nuclease-Free Duplex Buffer to the concentrations of 100  $\mu$ M. The two RNA oligos were diluted to 10  $\mu$ M final concentrations in a sterile microcentrifuge tube for a 10  $\mu$ l final volume, heated at 95°C for 5 min and allowed to be cool to room temperature on the bench top (5–10 min).

#### 3.6.3 Formation of the ribonucleoprotein (RNP) complex

The guide RNA (tubulin crRNA: tracrRNA duplex) and Cas9 enzyme were combined in that nucleofector solution to dilute each component to the final concentration 24 pmol in 50  $\mu$ l. The mixture was gently swirled using a pipet tip while pipetting and incubated at room temperature for 5-10 minutes.

### 3.6.4 Nucleofection

During the incubation time, BSS-iPSCs were prepared using StemPro Accutase Cell Dissociation Reagent (Thermo Fisher Scientific., USA.) to dissociate into single cells and counted to  $1 \times 10^6$  cells per electroporation. BSS-iPSCs were washed with 0.5% BSA (GE Healthcare, Austria), 2mM EDTA (Vivantis, Malaysia) in PBS and centrifuged at 1000 RPM for 5 minutes. The supernatant was removed as much as possible without disturbing the pellet. Fifty  $\mu$ l of nucleofection solution were added (P3 Primary Cell 4D-Nucleofector™ X Kit L, Lonza, Germany) to suspend cells. The RNP complex was co electroporated into the iPSCs cells along with a GFP donor plasmid specific to the target locus, AICSDP-4: TUBA1B-mEGFP (Addgene plasmid # 87421; <http://n2t.net/addgene:87421>; RRID: Addgene\_87421)

Nucleofection was performed using H9 program. The cells were then plated onto in 35 mm Matrigel-coated plate with CloneR™ medium (STEMCELL Technologies Inc., USA). GFP-expressed iPSCs were sorted by BD FACSAria II (Becton Dickinson, Franklin Lakes, NJ, USA).

### 3.7 Testing the effects of pharmacological agents on platelet production

In this study, iPSC lines from BSS patients were differentiated into MKs and platelets. The pharmacological agents, 15  $\mu$ M blebbistatin (Merck) or 50 ng/ml IL-1 $\alpha$  were added on day 19 and day 20 of MK differentiation, respectively. *In vitro*-derived platelets were stained for circumferential tubulin and measured the diameters (N = 500 per condition). Moreover, blebbistatin was combined with IL-1 $\alpha$  whereas Blebbistatin was added 72 hours before IL-1 $\alpha$ . *In vitro*-derived platelets were stained for circumferential tubulin and measured the diameters (N = 100 per condition

## CHAPTER IV

### RESULTS

#### 4.1 Generation of induced pluripotent stem cells (iPSCs) from Bernard Soulier syndrome (BSS) patients

Studies using human cells were approved by the institutional review board of the Faculty of Medicine of Chulalongkorn University and were conducted in accordance with the Declaration of Helsinki. Peripheral blood mononuclear cells (PBMCs) were obtained from two BSS patients and one unrelated normal individuals then reprogramming into iPSCs using nucleofection of episomal vectors.

BSS-iPSC lines were generated from 2 patients with BSS mutations in different genes (*GP1BA* and *GP1BB*: termed BSS-A and BSS-B, respectively). After reprogramming, we obtained 13 clones and 14 clones of BSS-A and BSS-B, successively. The BSS iPSC morphology showed the typical morphology of iPSCs that were compact colonies with defined borders, small cells with high nuclear to cytoplasmic ratio and prominent nucleoli. (Figure 4)

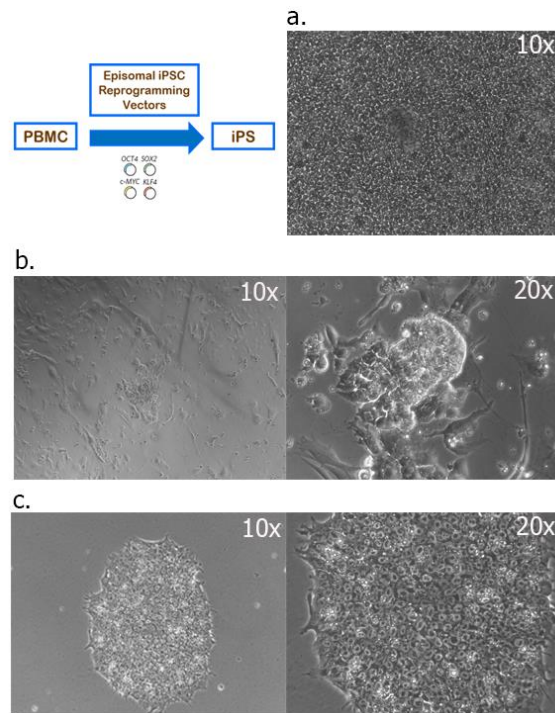


**Figure 4:** iPSCs reprogramming from PBMCs of BSS patients, (a.) PBMCs of BSS patients on MEF (DR4) feeder cell, (b.) iPSC colonies on day 10 after reprogramming, (c.) On day 14-21 after reprogramming, iPSC colonies were picked into a feeder free condition.

## 4.2 Characterization of iPSCs

### 4.2.1 Pluripotent stem cell markers expression by reverse-transcriptase polymerase chain reaction (RT-PCR)

To detect pluripotent gene expression of *OCT4*, *NANOG*, *SOX2*, *c-MYC* and *KLF-4* in BSS-iPSCs, RNAs obtained from clone No.1 of BSS-A-iPSCs and clone No.4 of BSS-B-iPSCs were subjected to PCR RT-PCR. The analysis revealed that the BSS-iPSCs expressed stem cell marker genes that were *OCT4*, *NANOG*, *SOX2*, *c-MYC* and *KLF-4*, similar to normal iPSCs. *GAPDH* gene as a housekeeping gene was also shown in the **Figure 5**.

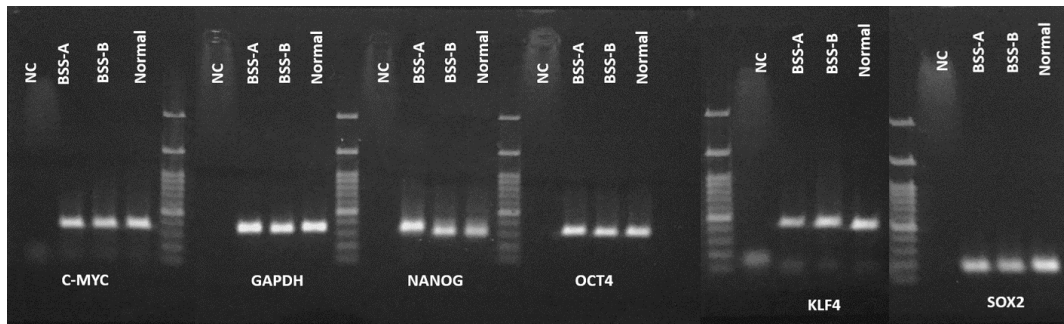


**Figure 5:** RT-PCR analysis of stem cell marker genes in BSS-A-iPSCs, SS-B-iPSCs and Normal iPSCs for expression of *OCT4*, *NANOG*, *SOX2*, *c-MYC*, *KLF-4* and *GAPDH*. NC indicated negative controls.

#### 4.2.2 *In vitro* differentiation of the iPSC lines

*In vitro* differentiating capacity of iPSCs was tested by spontaneous embryoid body (EB) differentiation. After dissociation of BSS iPSCs into small clumps, iPSCs formed EBs showing spherical shapes. EBs were grown for 7 days in floating culture and then seeded on gelatin-coated plate.

On day 7 of differentiation, there were cells migrating out of the EBs (**Figure 3**). EBs were cultured until day 21. After that, EBs were fixed and stained by immunofluorescence. Results showed that BSS iPSCs had the potential to differentiate into three germ layers by expressing the representative markers of ectoderm (NESTIN; NES), mesoderm (BRACHYURY; BRACHY) and endoderm (alpha-fetoprotein; AFP). (**Figure 4**)

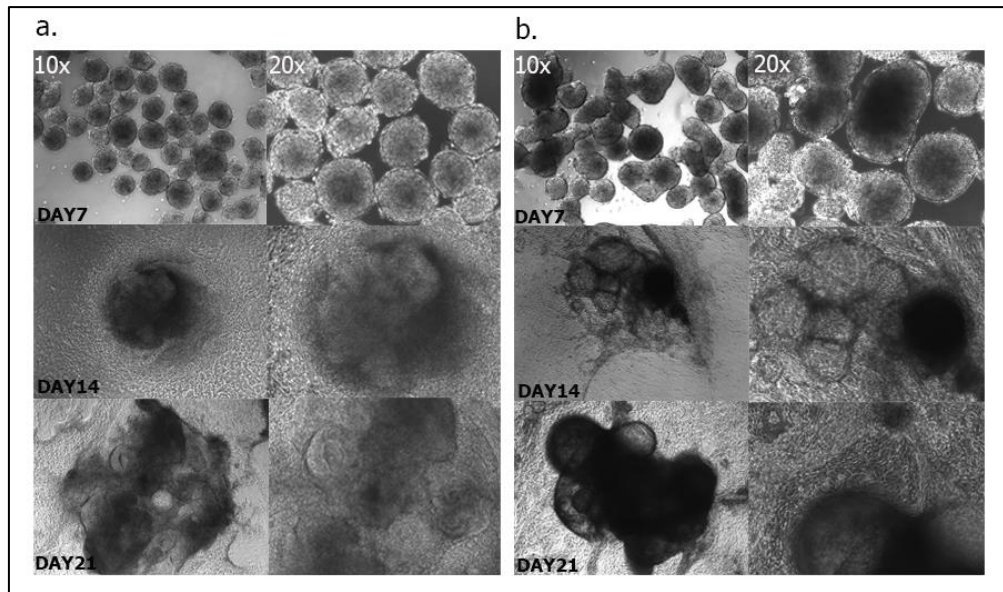


**Figure 6:** *In vitro* differentiation of BSS-A and BSS-B iPSCs: Embryoid body (EB) formation on DAY 7, 14 and 21 of BSS-A (a.) and BSS-B (b.)

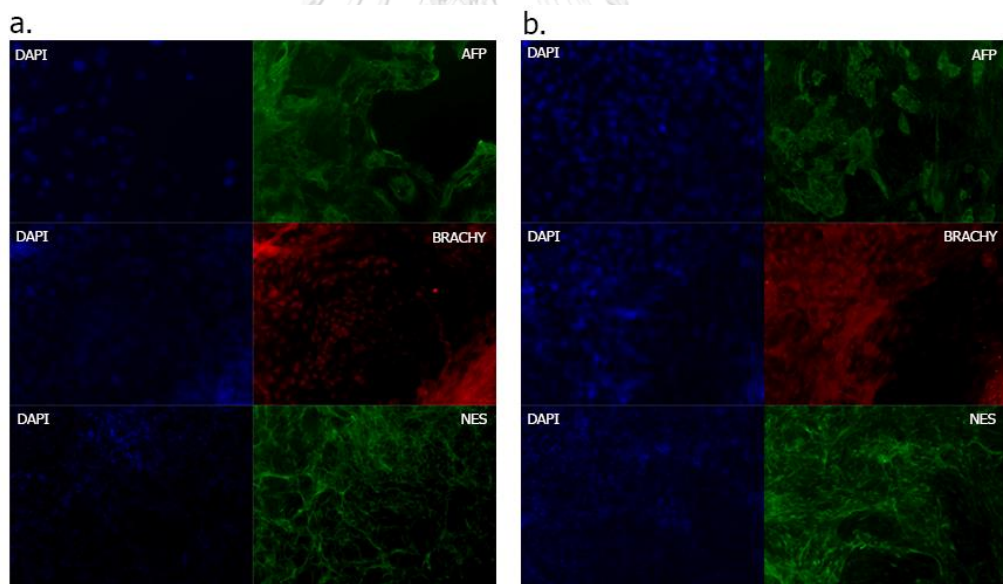


**Figure 7:** Immunofluorescence staining of endodermal (AFP), mesodermal (BRACHYURY) and ectodermal (NESTIN) markers of BSS-A (a.) and BSS-B (b.) embryoid bodies

#### 4.2.3 Immunocytochemistry for pluripotent cell markers

To characterize the pluripotent protein expression, Immunofluorescent staining of BSS-A-iPSCs (a.) and BSS-B iPSCs (b.) exhibited the expression of the intracellular pluripotency markers (OCT4 and NANOG) and cell surface pluripotency markers (SSEA4 and Tra-1-60).

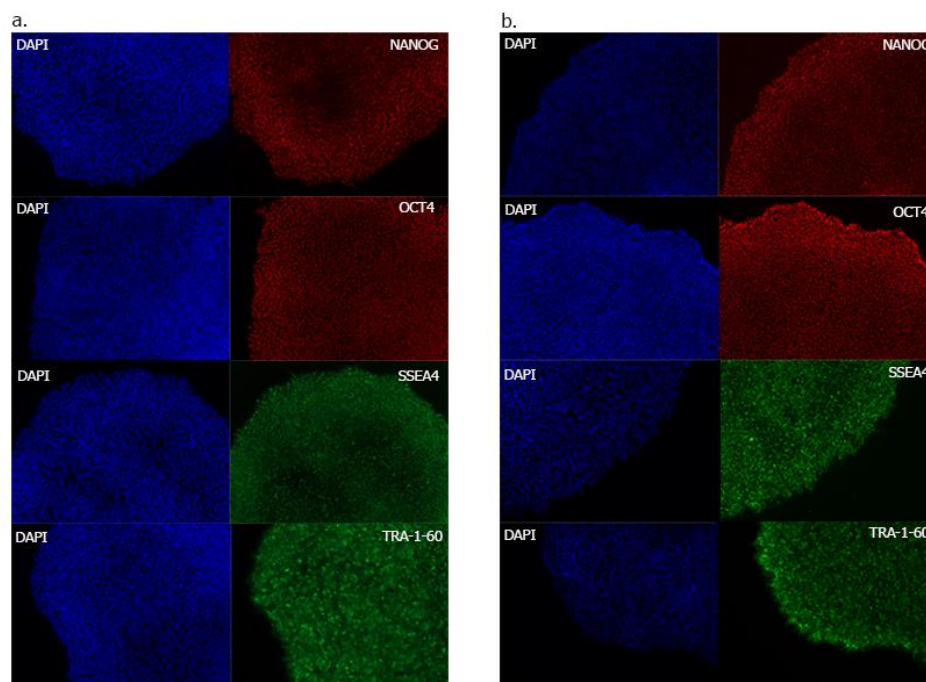


**Figure 8:** Immunocytochemistry (ICC) staining for the pluripotency protein markers OCT4, and NANOG, SSEA4 and TRA-1-60 in BSS-A iPSCs (a.) and BSS-B iPSCs (b.)



#### 4.2.4 Karyotyping

To confirm the intact karyotype after generation of iPSCs, metaphase chromosomes were analyzed. BSS-A-iPSCs and BSS-B iPSCs displayed a normal karyotype.

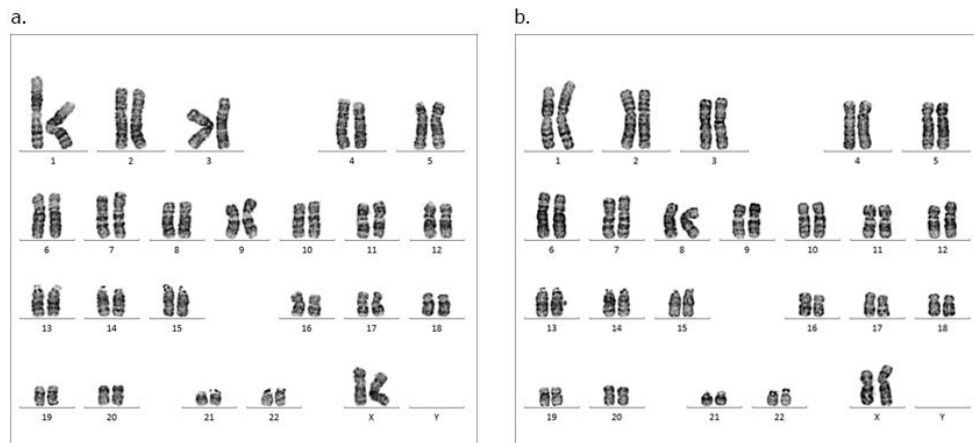


**Figure 9:** Metaphase karyotyping of BSS-A (a.) and BSS-B (b.)

#### 4.3 *In vitro* megakaryocyte and platelet differentiation via ES-Sacs method

To investigate whether the defect of BSS iPSC-derived megakaryocytes during maturation resemble phenotypes of patients' megakaryocytes, BSS-iPSCs were differentiated to megakaryocytes and platelets using ES-sacs method, according to the Takayama protocol. BSS-iPSCs were co-cultured with 10T1/2 feeder cells. On day 10-14 of differentiation, they showed a sac-like structure. After that the hematopoietic progenitors (HPCs) from ES-sacs (day 14) were harvested and stained for CD34. The result showed that HPCs inside in sacs expressed CD34, a hematopoietic stem cell marker. (**Figure 10**)

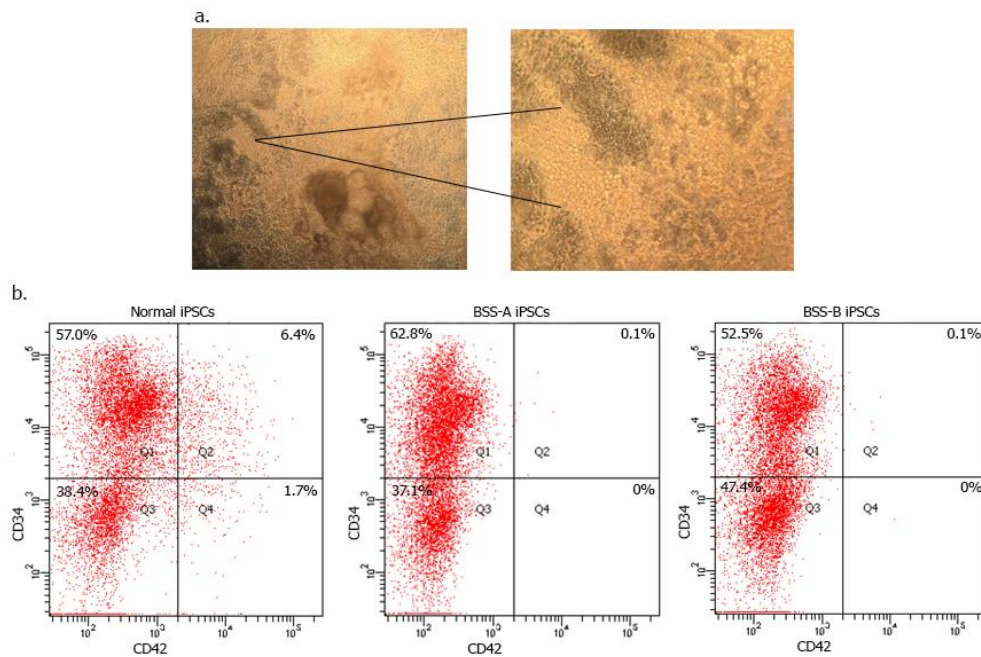


**Figure 10:** (a.) Upon ES-SAC differentiation, the sac-like structures were formed with hematopoietic progenitor cells (HPCs) inside (b.) On day 14 of differentiation, HPCs inside the sacs were harvested and stained for CD34. The normal, BSS-A and BSS-B iPSC-derived HPCs expressed CD34.

Subsequently, the CD34<sup>+</sup> cells were seeded on the OP9 marrow stromal cell line and after 5 days of culture (day 20 of differentiation), the CD41 and CD42 on megakaryocyte cell surface were analyzed by flow cytometry. The result showed that normal iPSC-derived megakaryocytes expressed CD41 and CD42 compared to BSS iPSC-derived megakaryocytes which expressed only CD41 similar to the patients' peripheral blood platelets. (**Figure 11a**)

To study BSS-iPSCs derived proplatelets and platelets' morphology. On day 20 of differentiation, BSS iPSC-derived megakaryocytes were harvested from the OP9 feeder and then seeded on Matrigel-coated coverslip.

On day 21, proplatelets formation were observed by staining with anti- $\alpha$ -tubulin antibody and anti-phalloidin antibody. Both BSS-A and BSS-B iPSC-derived proplatelets produced abnormal large proplatelets with thick shafts and tips compare to those of normal iPSC-derived proplatelets. (Figure 11b) The BSS iPSC-derived platelet diameters were measured on day 23 compared with normal iPSC-derived platelets (n=500). The result showed that BSS iPSCs produced abnormally large platelets with the diameters of  $4.34 \pm 0.043 \mu\text{m}$ ,  $3.88 \pm 0.045 \mu\text{m}$  and  $2.61 \pm 0.025 \mu\text{m}$  for BSS-A, BSS-B and normal iPSCs, respectively ( $p < 0.001$ ). (Figure 11c)

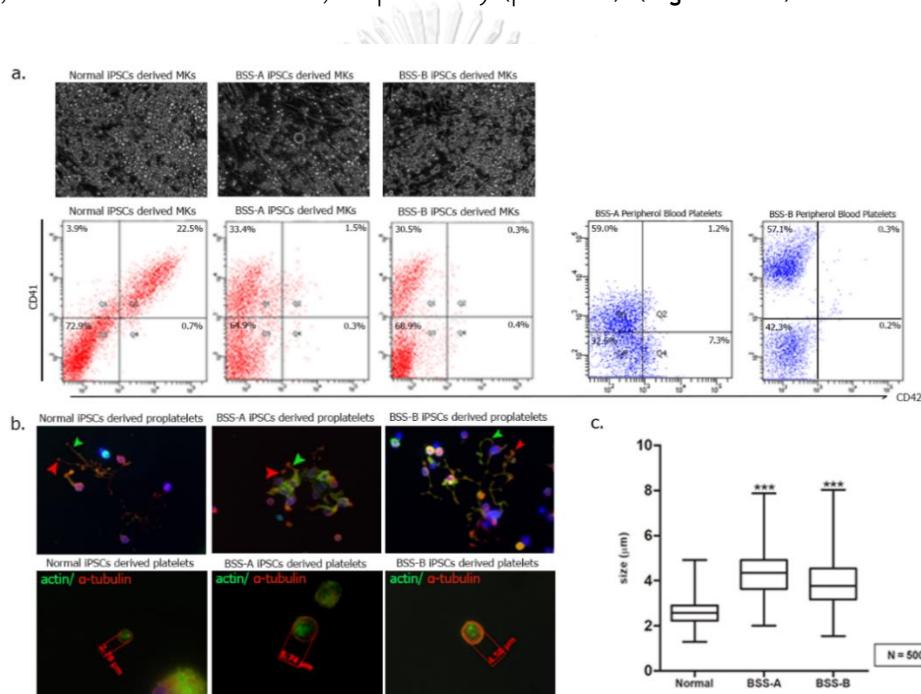


**Figure 11:** Megakaryocytes differentiation

(a.) On Day 20 of differentiation, MKs were harvested and tested for CD 41 and CD42b expression. Normal iPSC-derived MKs exhibited CD41 and CD42b compared to BSS-A and BSS-B iPSC-derived MKs which expressed only CD41. (b.) BSS-A and BSS-B iPSC-derived proplatelets exhibited the thick tips (red arrow) and thick shafts (green arrow) compared to normal iPSC-derived proplatelets. (c.) Platelets size determination showed BSS-A and BSS-B iPSC-derived platelets had significantly larger sizes compared to normal iPSC-derived platelets. (N=500)

#### 4.4 Genetic correction of BSS iPSCs and platelet sizes

BSS-A iPSCs were infected with lentivirus containing plvx-TRE3G-GP1BA vectors with plvx-EF1a-tet3G. Using the same method, BSS-B-iPSCs were infected with lentivirus containing plvx-TRE3G-*GP1BB* vectors with plvx-EF1a-tet3G. Then, both BSS-iPSCs were differentiated to megakaryocytes (MKs). The flow cytometry analysis on day 20 showed the expression of CD42 in BSS-A iPSC-derived MKs in the doxycycline induced condition compared with no doxycycline induction. (**Figure 12**) However, there was no expression of GPIb in BSS-B-iPSCs derived megakaryocytes. (**Figure 13**).

After that BSS-A-iPSCs derived megakaryocytes which expressed CD42b were separated for CD42-positive cells using magnetic separation method and differentiated to proplatelets and platelets. CD42<sup>+</sup>BSS-A iPSC-derived proplatelets exhibited normal proplatelet shafts and tips (**Figure 14a**) and platelets sizes were smaller than uncorrected BSS-A ( $3.184 \pm 0.078 \mu\text{m}$  [corrected BSS-A],  $4.453 \pm 0.096 \mu\text{m}$  [BSS-A],  $p < 0.001$ ) (n=100). (**Figure 14b**)

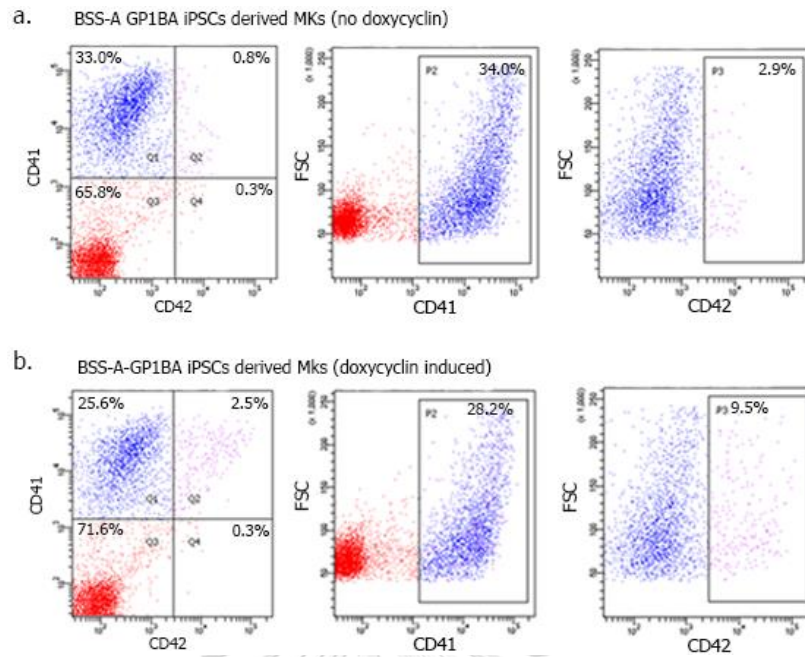


**Figure 12:** Flow cytometry analysis of corrected BSS-A iPSC-derived MKs without (a.) and with doxycyclin induced gene expression (b.)

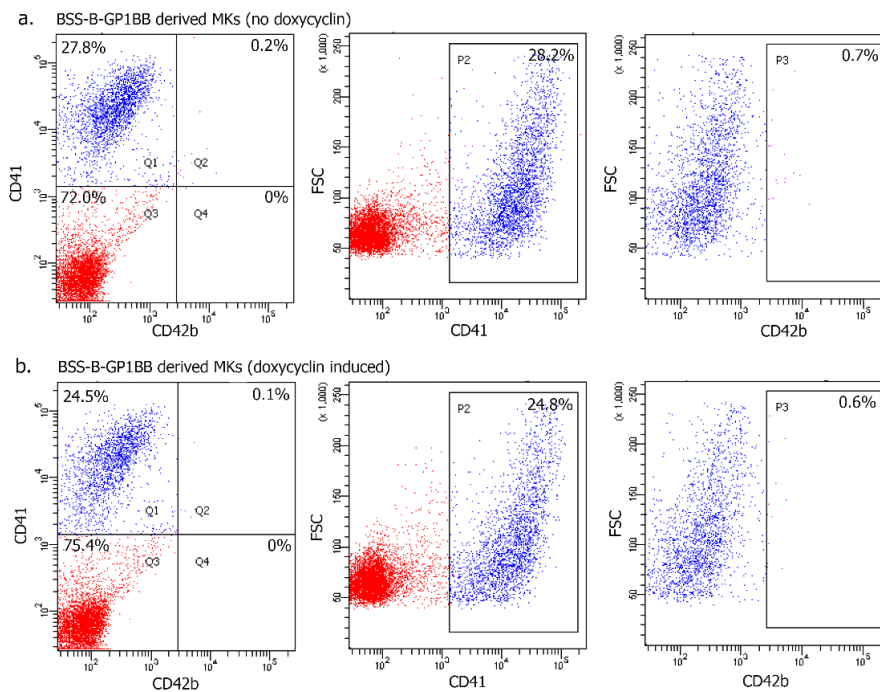


**Figure 13:** Flow cytometry analysis of corrected BSS-B iPSC-derived MKs without (a.) and with doxycyclin induced gene expression (b.)

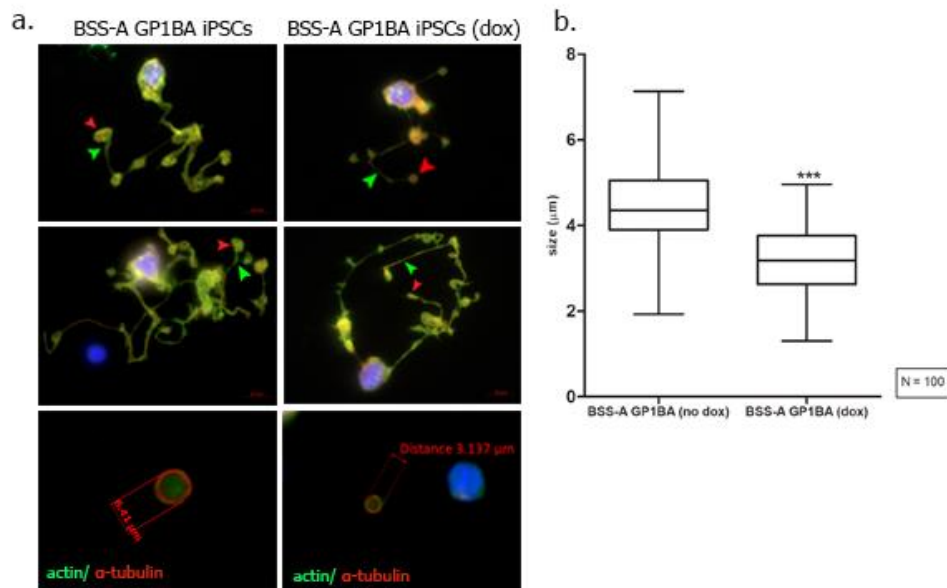


**Figure 14:** Proplatelet formation (a.) and platelets size determination (b.) of corrected BSS-A iPSC- derived proplatelets without and with doxycycline induced *GP1BA* gene expression

#### 4.5 Construction of iPSC with tubulin 1B alpha GFP reporter lines

To establish the iPSCs with tubulin green fluorescent protein (GFP) reporter line, the second exon of human tubulin alpha 1b chain (*TUBA1B*) was tagged with GFP fusion. After transfection with donor vector contained GFP-fused tubulin, BSS-iPSCs were cultured in 35 mm dish until cells were approximately 80-90% confluent. iPSCs were dissociated into single cell by ACCUTASE™ and GFP positive cells were sorted and collected by flow cytometer and sorter. GFP positive cells were seeded into the culture plate. After the BSS-iPSCs-tubulin GFP formed the colonies (**Figure 14**), BSS-iPSC with tubulin GFP was differentiated into megakaryocytes and proplatelets by the ES-SAC method. Result from the live image of iPSCs showed the expression of GFP which can be observed for the microtubule structure during their differentiating process to megakaryocytes and proplatelets. Therefore, we can obtain the BSS-iPSCs line with GFP tubulin expression as a tool to study proplatelet formation in the future (**Figure 15**).

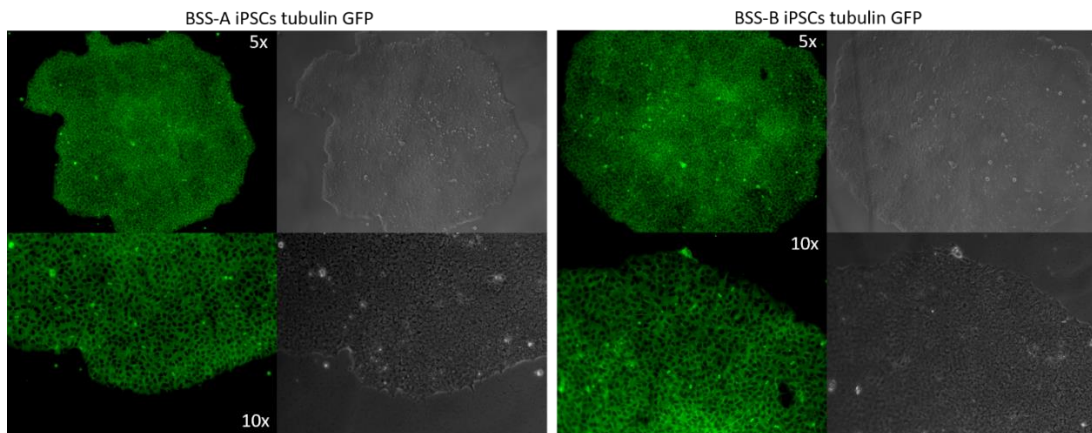


**Figure 15:** Live cell images of iPSCs with tubulin-GFP: BSS-A iPSCs (Left) and BSS-B iPSCs (Right)

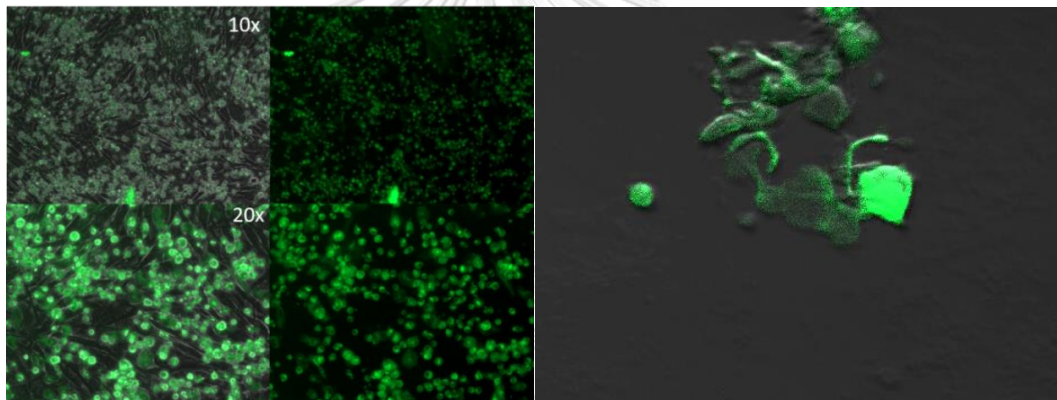


**Figure 16:** Live cells images of BSS iPSC-derived HPCs on OP9 feeder cell on Day 15 of ES-SAC differentiation (Left) and BSS iPSC-derived proplatelet on day 21 of ES-SAC differentiation (Right)

#### 4.6 Pharmacological agent effects on platelet formation *in vitro*

To study the effect of pharmacological agents on BSS platelet production, 50 ng/ml of IL-1 $\alpha$  was added BSS-derived megakaryocytes. The IL-1 $\alpha$ -induced MK rupture from normal iPSCs significantly yielded larger platelets with the platelet diameters  $2.643 \pm 0.026$  vs.  $3.262 \pm 0.038$  of normal culture without IL-1 $\alpha$  ( $p < 0.001$ ,  $N = 500$ ). However, there was no significant change in the sizes of BSS iPSCs-derived platelets in the presence or absence of IL-1 $\alpha$  ( $4.343 \pm 0.043$  vs  $4.322 \pm 0.047$ ,  $p = 0.74$  for BSS-A and

4.369±0.052 vs 4.223±0.059,  $p=0.06$  for BSS-B, N=500). (Figure 16a.) Furthermore, adding 15  $\mu\text{M}$  blebbistatin, a myosin II inhibitor, to BSS iPSC-derived MKs decreased the platelet sizes compared with the BSS cultures without blebbistatin. (3.20±0.035 vs. 4.38±0.046  $\mu\text{m}$  [BSS-A], 3.09±0.033 vs. 4.48±0.047  $\mu\text{m}$  [BSS-B],  $p<0.001$ ). (Figure 16b.) In addition, after added blebbistatin for 72 hours and then added IL-1 $\alpha$  in the presence of blebbistatin for 24 hours reveal the decreased size of BSS-iPSCs derived platelets compared to BSS-iPSCs derived platelet without blebbistatin and IL-1 $\alpha$  (4.43±0.110 vs. 3.34±0.090  $\mu\text{m}$  [BSS-A], 4.60±0.103 vs. 3.20±0.089  $\mu\text{m}$  [BSS-B],  $p<0.001$ , n=100) (Figure 16c.)

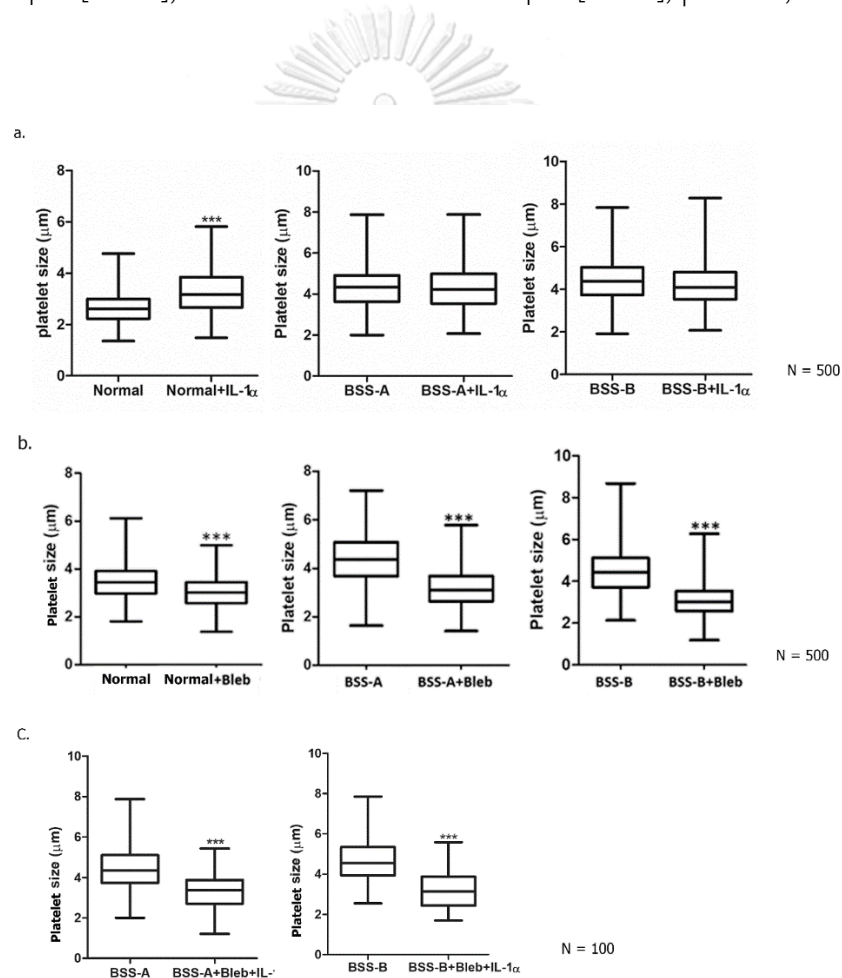


**Figure 17:** The determination of the mean sizes of iPSC-derived platelets from normal, BSS-A or BSS-B cultures (a.) In the absence or presence of IL-1 $\alpha$  and (b.) In the absence or presence of blebbistatin (c.) combined blebbistatin and IL-1 $\alpha$  condition



## CHAPTER V

### DISCUSSION

In this study, we generated a BSS model using patient-derived iPSCs technology recapitulating the disease phenotypes. BSS megakaryocytes derived from iPSCs did not express GPIb on cell surface and produced abnormally thick proplatelets shafts and tips. In addition, BSS platelets derived from iPSCs exhibited larger diameters compared with those derived from iPSCs.

In our study, we aim to correct the abnormal phenotype of BSS in iPSC disease model, the BSS-A-iPSCs were infected with the lentiviral vector containing the *GP1BA* gene and the BSS-B-iPSCs were infected with the lentiviral vector containing the *GP1BB* gene, after selection with antibiotics, the BSS-A iPSCs and BAA-B iPSCs which contained *GP1BA* and *GP1BB*, respectively, were differentiated into megakaryocytes and platelets. The doxycycline induced expression of GPIb in BSS-A-iPSCs with *GP1BA* derived megakaryocytes exhibited GPIb protein expression on megakaryocytes. Proplatelet morphology and platelets sizes became smaller compared to uncorrected BSS-iPSCs. However, the size of BSS iPSC-derived platelets did not decrease to the same size of normal iPSC-derived platelets probably caused by the low level of GPIb expression including with the CD42 positive cell separation step which may not isolate the pure population of CD42 positive cells.

Unlike BSS-A, BSS-B iPSCs with *GP1BB* derived megakaryocyte did not express GPIb on megakaryocytes in presence of doxycycline. No expression of GPIb protein on megakaryocytes derived from BSS-B iPSCs could be caused by poor infection efficiency or the improper amount of plvx-EF1a-Tet3G and plvx-TRE3G-*GP1BB* or mixed iPSC population which resulted in loss of inducibility after passaging. Reinfection or reselection of BSS-B iPSCs through single colony selection using selective

concentrations of puromycin and G418 may solve these problems. Moreover, DNA sequencing is needed to verify that the BSS-B iPSCs contain the transgenic *GP1BB*.

In conclusion, the correction of BSS-A iPSCs were consistent with the BSS animal models that showed that the transgenic expression of human GPIb in BSS could rescue platelets size and decrease tail bleeding time.<sup>9-12</sup> Although, the mouse model can represent some human BSS phenotypes but there are some limitations of the mouse models. For example, mouse models do not always demonstrate the same phenotypes as those observed in humans.<sup>13</sup>

In 2015, Nishimura *et al.*<sup>23</sup> reported that IL-1 $\alpha$ , an acute platelet releasing factor, released and induced MK membrane changes to produce platelets rapidly instead of the proplatelet formation pathway. This MK rupture process rapidly releases a large quantity of big but functional platelets in case of acute inflammation or an acute platelet need. To investigate platelet production via this pathway, based on this previously reported experiment, IL-1 $\alpha$  was added during MK differentiation from BSS and normal iPSCs. The result showed that there was no difference in size of BSS-iPSCs derived platelets with or without IL-1 $\alpha$  suggesting that the mechanism of BSS large platelet biogenesis did not involve the IL-1 $\alpha$ -MK rupture pathway.

MK cytoskeleton plays vital roles in proplatelet formation and platelet size controls as mutations in cytoskeleton or cytoskeletal binding proteins result in various kinds of hereditary macrothrombocytopenia. Spinler *et al.*<sup>50</sup> reported that blebbistatin, which is a myosin II inhibitor, involved in myosin II activity affecting MK membrane fragmentation from large to normal sizes of pre-/pro-platelets. Myosin has been reported to destabilize microtubules marginal bands that maintain resting platelet discoid shape<sup>33</sup> via contraction of actomyosin structures.<sup>4</sup> Therefore, inhibition of myosin II by blebbistatin stabilized microtubules.<sup>51</sup> Notably, it also caused giant platelets of MYH-9 disorders to become significantly smaller.<sup>52</sup> Our experiment also demonstrated that the mean sizes of normal iPSC- and BSS iPSC-derived platelets were

significantly decreased. From another experiment, in which blebbistatin was added for 72 hours then combined with IL-1 $\alpha$  for 24 hours, also exhibited the decreased sizes of BSS iPSC--derived platelets. Therefore, blebbistatin still inhibited myosin II activity in the presence of IL-1 $\alpha$ .

These data suggested that GPIb-IX-V was likely involved in the proplatelet formation not the MK rupture. However, both pathways were related to an inhibition of myosin function. It is important to note that the experimental models of both MYH9 disorders and BSS were performed in the culture system without any shear stress. The condition is different from the native *in vivo* environment.

Recently, there are many studies that use fluorescent protein reporter to investigate the mechanism of platelet production. For instance, MKs maturation was monitored by using  $\beta$ 1 tubulin venus reporter line, which provided the system for high-throughput drug screening.<sup>53</sup> In our study, we successfully established a BSS-iPSC reporter line, which expressed tubulin-GFP fusion protein. This reporter line is the useful tool, which enables us to visualize the different stages in proplatelet maturation and platelet release including cytoskeletal rearrangements in order to elucidate the pathogenesis of giant platelet disorders.

In summary, the iPSC is a good model of platelet production in BSS patients. In the future studies, this system may be used to explore the pathogenesis of other forms of macrothrombocytopenia and screen for novel therapeutic strategies for diseases of platelet production.

## REFERENCES

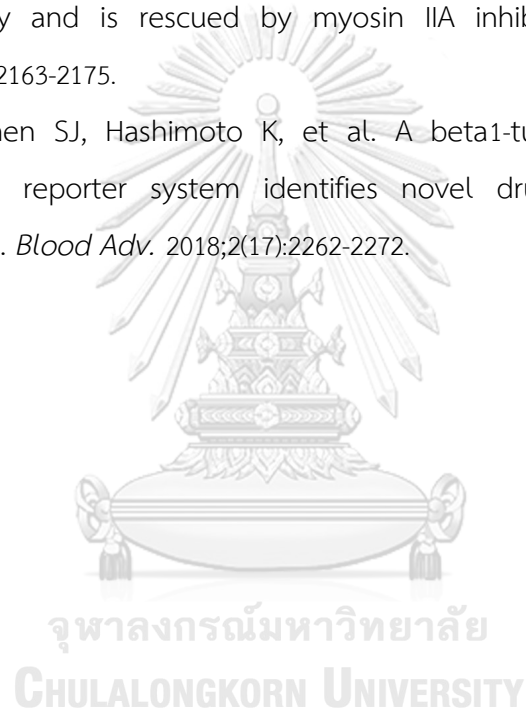
1. Berndt MC, Andrews RK. Bernard-Soulier syndrome. *Haematologica*. 2011;96(3):355-359.
2. Patel SR, Hartwig JH, Italiano JE, Jr. The biogenesis of platelets from megakaryocyte proplatelets. *J Clin Invest*. 2005;115(12):3348-3354.
3. Lanza F. Bernard-Soulier syndrome (hemorrhagic thrombocytopenic dystrophy). *Orphanet J Rare Dis*. 2006;1:46.
4. Michelson AD. *Platelets*. Elsevier Science; 2013.
5. Andrews RK, Berndt MC. Bernard-Soulier syndrome: an update. *Semin Thromb Hemost*. 2013;39(6):656-662.
6. Kanaji T, Ware J, Okamura T, Newman PJ. GPIIb/IIIa regulates platelet size by controlling the subcellular localization of filamin. *Blood*. 2012;119(12):2906-2913.
7. Jurak Begonja A, Hoffmeister KM, Hartwig JH, Falet H. FlnA-null megakaryocytes prematurely release large and fragile platelets that circulate poorly. *Blood*. 2011;118(8):2285-2295.
8. Simon DI, Chen Z, Xu H, et al. Platelet glycoprotein IIb/IIIa is a counterreceptor for the leukocyte integrin Mac-1 (CD11b/CD18). *The Journal of experimental medicine*. 2000;192(2):193-204.
9. Ware J, Russell S, Ruggeri ZM. Generation and rescue of a murine model of platelet dysfunction: the Bernard-Soulier syndrome. *Proc Natl Acad Sci U S A*. 2000;97(6):2803-2808.
10. Strassel C, Eckly A, Leon C, et al. Intrinsic impaired proplatelet formation and microtubule coil assembly of megakaryocytes in a mouse model of Bernard-Soulier syndrome. *Haematologica*. 2009;94(6):800-810.
11. Kanaji S, Kuether EL, Fahs SA, et al. Correction of murine Bernard-Soulier syndrome by lentivirus-mediated gene therapy. *Mol Ther*. 2012;20(3):625-632.
12. Strassel C, Bull A, Moog S, et al. Lentiviral gene rescue of a Bernard-Soulier mouse model to study platelet glycoprotein IIb/IIIa function. *J Thromb Haemost*. 2016;14(7):1470-1479.

13. Cibelli J, Emborg ME, Prockop DJ, et al. Strategies for improving animal models for regenerative medicine. *Cell Stem Cell*. 2013;12(3):271-274.
14. Machlus KR, Italiano JE, Jr. The incredible journey: From megakaryocyte development to platelet formation. *J Cell Biol*. 2013;201(6):785-796.
15. Pease DC. An electron microscopic study of red bone marrow. *Blood*. 1956;11(6):501-526.
16. Nakeff A, Maat B. Separation of megakaryocytes from mouse bone marrow by velocity sedimentation. *Blood*. 1974;43(4):591-595.
17. Italiano JE, Jr., Shivdasani RA. Megakaryocytes and beyond: the birth of platelets. *J Thromb Haemost*. 2003;1(6):1174-1182.
18. Ebbe S, FSJ. Megakaryocytopoiesis in the rat. *Blood*. 1965;26:20-35.
19. Odell TTJ, C.W. Jackson. Polyploidy and maturation of rat megakaryocytes. *Blood*. 1968;32:102-110.
20. Odell TTJ, C.W. Jackson, T.J. Friday. Megakaryocytopoiesis in rats with special reference to polyploidy. *Blood*. 1970;35:775-782.
21. Takayama N, H. Nishikii, J. Usui, et al. Generation of functional platelets from human embryonic stem cells in vitro via ES-sacs, VEGF-promoted structures that concentrate hematopoietic progenitors. *blood*. 2008;111:5298-5306.
22. Nieswandt B, Stritt S. Megakaryocyte rupture for acute platelet needs. *J Cell Biol*. 2015;209(3):327-328.
23. Nishimura S, Nagasaki M, Kunishima S, et al. IL-1alpha induces thrombopoiesis through megakaryocyte rupture in response to acute platelet needs. *J Cell Biol*. 2015;209(3):453-466.
24. Aster RH. Studies of the mechanism of hypersplenic thrombocytopenia in rats. *J Lab Clin Med*. 1967;70:736-751.
25. Harker LA, Finch CA. Thrombokinetis in man. *J Clin Invest* 1969;48:963-974.
26. Jackson CW, Edwards CC. Biphasic thrombopoietic response to severe hypobaric hypoxia. *Br J Haematol*. 1977; 35:233-244.
27. Bender M, Thon JN, Ehrlicher AJ, et al. Microtubule sliding drives proplatelet elongation and is dependent on cytoplasmic dynein. *Blood*. 2015;125(5):860-868.

28. Thon JN, Italiano JE, Jr. Does size matter in platelet production? *Blood*. 2012;120(8):1552-1561.
29. Daniel JL, Molish IR, Rigmaiden M, Stewart G. Evidence for a role of myosin phosphorylation in the initiation of the platelet shape change response. *J Biol Chem*. 1984;259(15):9826-9831.
30. Klages B, Brandt U, Simon MI, Schultz G, Offermanns S. Activation of G12/G13 results in shape change and Rho/Rho-kinase-mediated myosin light chain phosphorylation in mouse platelets. *J Cell Biol*. 1999;144(4):745-754.
31. Retzer M, Essler M. Lysophosphatidic acid-induced platelet shape change proceeds via Rho/Rho kinase-mediated myosin light-chain and moesin phosphorylation. *Cell Signal*. 2000;12(9-10):645-648.
32. Shin EK, Park H, Noh JY, Lim KM, Chung JH. Platelet Shape Changes and Cytoskeleton Dynamics as Novel Therapeutic Targets for Anti-Thrombotic Drugs. *Biomol Ther (Seoul)*. 2017;25(3):223-230.
33. Diagouraga B, Grichine A, Fertin A, Wang J, Khochbin S, Sadoul K. Motor-driven marginal band coiling promotes cell shape change during platelet activation. *J Cell Biol*. 2014;204(2):177-185.
34. Schulze H, R.A. Shivdasani Mechanisms of thrombopoiesis. *J Thromb Haemost* 2005;3:1717-1724.
35. Junt T, H. Schulze, Z. Chen, et al. Dynamic visualization of thrombopoiesis within bone marrow. *Science*. 2007;317:1767-1770
36. Shivdasani RA, Orkin. SH. Erythropoiesis and globin gene expression in mice lacking the transcription factor NF-E2. *Proc Natl Acad Sci USA*. 1995;92:8690-8694.
37. Mikkola HK, J. Klintman, H. Yang HH, T.M. Schlaeger, Y. Fujiwara, Orkin SH. Haematopoietic stem cells retain long-term repopulating activity and multipotency in the absence of stem-cell leukaemia SCL/tal-1 gene. *Nature*. 2003; 421:547-551.
38. Kaushansky K. The molecular mechanisms that control thrombopoiesis. *J Clin Invest*. 2005; 115:3339-3347.
39. Gaur M, T. Kamata, S. Wang, B. Moran, S.J. Shattil, Leavitt AD. Megakaryocytes derived from human embryonic stem cells: a genetically tractable system to

- study megakaryocytopoiesis and integrin function. *J Thromb Haemost.* 2006;4:436-442.
40. Stenberg PE, Levin. J. Mechanisms of platelet production. *Blood Cells.* 1989;15:23-47.
41. Takayama N, S. Nishimura, S. Nakamura, et al. Transient activation of c-MYC expression is critical for efficient platelet generation from human induced pluripotent stem cells. *J Exp Med.* 2010;207:2817-2830.
42. Takayama N, Eto K. In vitro generation of megakaryocytes and platelets from human embryonic stem cells and induced pluripotent stem cells. *Methods Mol Biol.* 2012;788:205-217.
43. Hirata S, Takayama N, Jono-Ohnishi R ea. Congenital amegakaryocytic thrombocytopenia iPS cells exhibit defective MPL-mediated signaling. *J Clin Invest.* 2013;123:3802-3814.
44. Sullivan SK, Mills JA, Koukouritaki SB ea. High-level transgene expression in induced pluripotent stem cell-derived megakaryocytes: correction of Glanzmann thrombasthenia. *blood.* 2013;123:753-757.
45. Carver-Moore K, Broxmeyer HE, Luoh SM ea. Low levels of erythroid and myeloid progenitors in thrombopoietin-and c-mpl-deficient mice. *Blood.* 1996;88:803-808.
46. Ingrungruanglert P, Amarinthnukrowh P, Rungsiwiwut R, et al. Wiskott-Aldrich syndrome iPS cells produce megakaryocytes with defects in cytoskeletal rearrangement and proplatelet formation. *Thromb Haemost.* 2015;113(4):792-805.
47. Lu SJ, Luo C, Holton K, Feng Q, Ivanova Y, Lanza R. Robust generation of hemangioblastic progenitors from human embryonic stem cells. *Regen Med.* 2008;3(5):693-704.
48. Takahashi K, Tanabe K, Ohnuki M, et al. Induction of pluripotent stem cells from adult human fibroblasts by defined factors. *Cell.* 2007;131(5):861-872.
49. Roberts B, Haupt A, Tucker A, et al. Systematic gene tagging using CRISPR/Cas9 in human stem cells to illuminate cell organization. *Mol Biol Cell.* 2017;28(21):2854-2874.

50. Spinler KR, Shin JW, Lambert MP, Discher DE. Myosin-II repression favors pre/proplatelets but shear activation generates platelets and fails in macrothrombocytopenia. *Blood*. 2015;125(3):525-533.
51. Takesono A, Heasman SJ, Wojciak-Stothard B, Garg R, Ridley AJ. Microtubules regulate migratory polarity through Rho/ROCK signaling in T cells. *PLoS One*. 2010;5(1):e8774.
52. Chen Y, Boukour S, Milloud R, et al. The abnormal proplatelet formation in MYH9-related macrothrombocytopenia results from an increased actomyosin contractility and is rescued by myosin IIA inhibition. *J Thromb Haemost*. 2013;11(12):2163-2175.
53. Seo H, Chen SJ, Hashimoto K, et al. A beta1-tubulin-based megakaryocyte maturation reporter system identifies novel drugs that promote platelet production. *Blood Adv*. 2018;2(17):2262-2272.







จุฬาลงกรณ์มหาวิทยาลัย  
**CHULALONGKORN UNIVERSITY**

## VITA

**NAME** Ponthip Mekchay

**DATE OF BIRTH** 12 July 1983

**PLACE OF BIRTH** Thailand

**INSTITUTIONS ATTENDED** Graduate School, Biomedical Sciences

**HOME ADDRESS** 77/71 Ratchathewee Tower , Phayathai Rd.,  
Ratchathewee, Bangkok. 10400

**PUBLICATION** Mekchay, Ponthip & Rojnuckarin, Ponlapat. (2012).  
Molecular cloning and characterization of alboaggregin D,  
a novel platelet activating protein, from Green pit viper  
(Cryptelytrops albolabris) venom. *Toxicon* : official journal  
of the International Society on Toxinology. 59. 59-67.  
10.1016/j.toxicon.2011.10.009.

**AWARD RECEIVED** Travel Grant Award in the 10th Congress for the Asian-  
Pacific Society on Thrombosis and Hemostasis (APSTH) on  
June 28 (Thu.) - 30 (Sat.), 2018 at Royton Sapporo, Japan.